Running coupling constant in thermal ϕ^4 theory up to two loop order

K. Arjun,* A. M. Vinodkumar, and Vishnu Mayya Bannur
Department of Physics, University of Calicut, Kerala 673635, India

(Received 5 April 2021; revised 6 September 2021; accepted 9 December 2021; published 27 January 2022)

Using the imaginary time formalism in thermal field theory, we derive the running coupling constant and running mass in two loop order. In the process, we express the imaginary time formalism of Feynman diagrams as the summation of nonthermal quantum field theory (QFT) Feynman diagrams with coefficients that depend on temperature and mass. Renormalization constants for thermal ϕ^4 theory were derived using simple diagrammatic analysis. Our model links the nonthermal QFT and the imaginary time formalism by assuming both have the same mass scale μ and coupling constant g. When these results are combined with the renormalization group equations and applied simultaneously to thermal and nonthermal proper vertex functions, the coupling constant and running mass with implicit temperature dependence are obtained. We evaluated pressure for scalar particles in two loop orders at the zero external momentum limit by substituting the running mass result in the quasiparticle model.

DOI: 10.1103/PhysRevD.105.025023

I. INTRODUCTION

There are different quasiparticle models [1–9] used to describe the state of the quark-gluon plasma (QGP). Many of these models depend upon the corresponding running coupling constant. Therefore the nature of the coupling constant and associated renormalization group equations (RGE) were always exciting topics in quantum field theory.

Using the renormalization group equation, Collins and Perry [10] published a significant study on ultradense nuclear matter (the idea of quark soup at high density) in 1975. The concept of thermally dependent RGEs [11,12] considered the mass and the coupling constant as temperature functions. In deriving the coupling constant, changes in the vertex function results in variations in the coupling constant [13,14]. This means the coupling constant has a strong dependence on the vertex function [15,16]. Also, the dependence of the coupling constant on the gauge was investigated in [17,18]. Braaten and Pisarski [19] introduced significant ideas such as hard thermal loops and, using it, they presented the resummation of quantum chromodynamics (QCD) thermal perturbation theory. A perturbative analysis of QCD at the static limit was shown in [20]. The authors used both momentum and temperature-dependent RGEs and derived a coupling constant that depends on momentum scale and temperature. During the same decade, several renormalization concepts were introduced, including environment friendly renormalization [21,22] and the idea of using more than one renormalization group for running mass and temperature [23,24]. Recent developments include the research on magnetic field effects on the coupling constant and the expression for the thermomagnetic coupling constant at one loop order [25,26].

On the description of QGP [3–7,27], most of the models take readily available coupling constants [28] from QCD and evaluate their results. The most famous coupling constants in QCD have inverse logarithmic [29,30] thermal dependency. Steffens [31] investigates the nonlogarithmic and logarithmic nature of the QCD coupling of the high-temperature limit. We can find works related to quark dynamics in a magnetic field that apply magnetic field-dependent coupling constants [25,26] in quasiparticle models [8,9,32,33] to determine the equation of state. These models consider quarks and gluons as quasiparticles with thermal mass depending on various parameters such as the coupling constant, temperature, and magnetic field.

In the context of nonthermal and thermal field theory, we pay special attention to the quartic (ϕ^4) interaction (also known as the toy model) theory for two loop order. In this work, we use the simple diagrammatic analysis [34] in imaginary time formalism (ITF) [35] to derive a coupling constant that obeys RGE for both thermal and nonthermal field theories under the same mass scale μ and coupling constant g. We take advantage of the analytically consistent theory [36], evaluated at the external momentum equal to zero. We can extend the same approach to QCD.

The self-energy part of the quartic interaction tadpole can be found in papers [37–41] under various approximations such as massive and massless Lagrangian density. The

*arjunk_dop@uoc.ac.in

authors of [39,42] calculate the free energy part of the ϕ^4 interactions, and [43] contains the higher-order calculations. In our work, we define Lagrangian density as

$$\mathcal{L} = \frac{1}{2}\{\partial_\mu\phi\partial^\mu\phi - m^2\phi^2\} - \frac{\lambda}{4!}\phi^4 \tag{1}$$

and follow a systematic approach (λ is the nonrenormalized coupling constant). The Lagrangian density is massive itself and consists of a quadratic and quartic interaction term. Some of the Feynman diagram integral results and formulas derived and used in this work may be found in other publications [34,35,44–46]. We employ the dimensional regularization method [47–49], which successfully regularizes non-Abelian gauge theory while preserving symmetries. The minimal subtraction scheme (MS scheme) follows after regularization, in which it corresponds to canceling out the pole parts (ϵ) through the method of counterterms [50]. Then we apply the corresponding RGE to finite proper vertex function (FPVF) in imaginary time formalism in which the removal of divergences at $\epsilon \to 0$, and the vertex function becomes finite 54–51]].

In this work, we use subscripts QFT (quantum field theory) and ITF to represent Feynman diagrams expressed in *nonthermal QFT* and *imaginary time formalism*. Abbreviations TLA, SMC, and FPVF, represent for the "two loop approximation", the "same mass scale (μ) and coupling constant (g)", and "finite proper vertex function", respectively. Throughout this paper, we used Euclidean momentum $K = [\omega_{n_k}, k]$ to write $K^2 = \omega_{n_k}^2 + k^2$. One can see three β's appearing in this work. β denotes $1/T$. $\beta(g)$ denotes the beta function associated with RGE. β_2 and β_3 are the coefficients of g^2 and g^3 of the beta function, respectively.

In the RGE, we have an equation connecting the coupling constant with the mass scale using $\beta(g) = \frac{dg}{d\ln\mu}$ and an equation connecting the running mass with mass scale $\gamma_m(g) = \frac{d\ln m}{d\ln\mu}$. In thermal and nonthermal field theories, $\beta(g)$ and $\gamma_m(g)$ have the same expression. Suppose we have an additional equation connecting the coupling constant with temperature. With the help of $\beta(g), \gamma_m(g)$, and this new temperature-dependent equation, it is possible to find the temperature-dependent running mass, mass scale, and coupling constant.

We introduce a new approach where we apply RGE simultaneously on thermal and nonthermal FPVF under SMC. It results in a polynomial expression in g of order four. After a close examination, one can find that coefficients of g^2, g, g^0 are zero. So the nontrivial solution reduces to a linear equation in g with coefficients that depend on running mass, temperature, and mass scale. A minor rearrangement brings out the relation between coupling, running mass, temperature, and mass scale.

We follow a systematic approach [34]. To ease the calculation, we make relations between diagrams in thermal and nonthermal field theories. We try to express all the ITF diagrams as the sum of QFT diagrams with thermal coefficients.

In Sec. II, we write down all essential diagrams, such as two- and four-point functions in one and two loop order, in ITF and QFT. We express ITF diagrams as sums of QFT diagrams (with and without thermal coefficients). We derive the requisite counterterm diagrams in Sec. III to remove the divergences from the corresponding proper vertex function and derive renormalization constants in ITF. In Sec. IV, we calculate renormalization constants through necessary diagrams. Section V discusses the idea and outcome of applying RGE on the FPVF difference and how it will lead to the temperature-dependent coupling constant under SMC. Section VI includes plots revealing the temperature relations, such as the coupling constant vs temperature, running mass vs temperature, mass scale vs temperature, and pressure vs temperature. In Sec. VI, we verify the qualitative behavior of running mass and coupling results. We substitute the running mass on the self-consistent quasiparticle model [5–7] pressure relation and check whether it will lead to the Stephen-Boltzmann limit at the higher temperature approximations.

Another essential nature is the flexibility of this model. It depends on the integration constants and functions $\beta(g)$ and $\gamma_m(g)$. Once we have data points, we can fit running mass, coupling, pressure results to the data points by choosing appropriate values for the integral constants.

II. REGULARIZATION

It is possible to write down all diagrams in the ϕ^4 theory by a set of fundamental nontrivial Feynman diagrams known as one-particle irreducible (1 PI) diagrams. In other words, they are the smallest building block of diagrams:

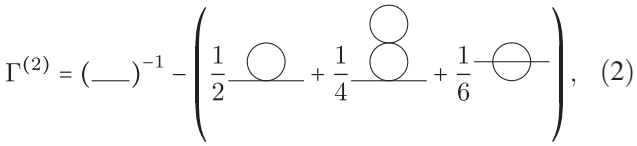

(2)

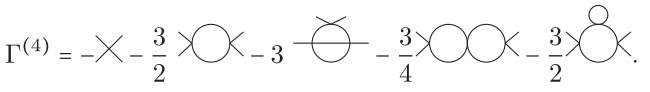

(3)

Equations (2) and (3) are two- and four-point vertex functions, expressed using corresponding 1 PI diagrams.

In ϕ^4 ITF and nonthermal QFT, both these two- and four-point functions and their corresponding integrals diverge. We follow the dimensional regularization procedure in which we introduce a parameter to pinpoint the diverging term and separate the singularity [47–49]. In Secs. II A and II B, we express the two- and four-point vertex functions in ITF as the summation of corresponding nonthermal QFT vertex

functions with thermal coefficients. In the following evaluations, the remaining $g\mu^\epsilon$ will become $\lambda \approx g$ at $\epsilon \to 0$. Similarly in the case of finite terms, $\lambda^2 \to (g\mu^\epsilon)^2 \approx g^2$ as $\epsilon \to 0$.

A. One loop order diagrams

1. Two-point function

We define the tadpole diagram in imaginary time formalism as

$$= -\lambda\, T \sum_n \int \frac{1}{p^2 + m^2 + \omega_n^2} \frac{d^3p}{(2\pi)^3} \tag{4}$$

and that of nonthermal ϕ^4 theory as

$$= -\lambda \int \frac{1}{p^2 + m^2} \frac{d^4p}{(2\pi)^4}, \tag{5}$$

and we use the result from Appendix A-1 and express tadpole in ITF in terms of tadpole in nonthermal QFT as

$$= \text{ 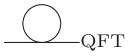 } - \lambda S_1(m,T), \tag{6}$$

where

$$S_1(m,T) = \int \frac{n_B(\beta\epsilon_p)}{\epsilon_p} \frac{d^3p}{(2\pi)^3} = \frac{1}{\pi} \sum_{n=1}^{\infty} \left(\frac{m}{2\pi n\beta}\right) K_1(n\beta m). \tag{7}$$

We can describe the divergence as a singularity of parameter ϵ by substituting $\lambda = g\mu^\epsilon$ at dimension N (say) to $N - \epsilon$. We get the regularization result

$$= \frac{m^2 g}{(4\pi)^2}\left[\frac{2}{\epsilon} + \psi(2) + \ln\left(\frac{4\pi\mu^2}{m^2}\right)\right] - g\mu^\epsilon S_1(m,T) + \mathcal{O}(\epsilon), \tag{8}$$

in which $\psi(n)$ is the Euler Digamma function, g is the dimensionless coupling constant, and $n_B(x) = (e^x - 1)^{-1}$. As $\epsilon \to 0$, the first term diverges.

2. Four-point function

The four-point function diagram definition for one loop order is

$$= \int \frac{d^3p}{(2\pi)^3} \sum_{n_p=-\infty}^{\infty} \frac{\lambda^2 T}{\omega_{n_p}^2 + \varepsilon_p^2} \frac{1}{\omega_{n_p - n_q}^2 + \varepsilon_{p-q}^2} \tag{9}$$

with $\varepsilon_p^2 = p^2 + m^2$ (diagram is also known as scattering diagram). The corresponding diagram in the nonthermal QFT is

$$= \int \frac{d^4P}{(2\pi)^4} \frac{\lambda^2}{P^2 + m^2} \frac{1}{(P-Q)^2 + m^2}. \tag{10}$$

One can relate these two diagrams after regularization ($\lambda \to g\mu^\epsilon, \frac{d^3p}{(2\pi)^3} \to \frac{d^{3-\epsilon}p}{(2\pi)^{3-\epsilon}}, \frac{d^4p}{(2\pi)^4} \to \frac{d^{4-\epsilon}p}{(2\pi)^{4-\epsilon}}$) as shown in Appendix A-2 as

$$= \text{  } + (g\mu^\epsilon)^2 W(q, n_q) \tag{11}$$

with

$$W(r,n_r) = \int \frac{2n_B(\beta\varepsilon_p)(r^2 + 2pr\cos\theta + \omega_{n_r}^2)}{\varepsilon_p((r^2 + 2pr\cos\theta + \omega_{n_r}^2)^2 + 4\varepsilon_p^2\omega_{n_r}^2)} \frac{d^3p}{(2\pi)^3}. \tag{12}$$

Using dimensional regularization ($\lambda = g\mu^\epsilon$) and standard textbook results [34], we can write

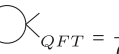

$$= \frac{g^2\mu^\epsilon}{(4\pi)^2}\left(\frac{2}{\epsilon} + \psi(1) + \int_0^1 dx \ln\left[\frac{4\pi\mu^2}{Q^2x(1-x) + m^2}\right]\right) + \mathcal{O}(\epsilon) \tag{13}$$

with $Q = [\omega_{n_q}, \vec{q}]$.

The external momentum $\vec{k}$ is the sum of the incoming momenta $\vec{k}_1 + \vec{k}_2$ and the Matsubara summation parameter $\omega_{n_k} = \omega_{n_{k_1}} + \omega_{n_{k_2}}$, where $\omega_{n_k} = 2\pi n_k T$ with n_k being an integer. For Matsubara summation, we use the symbol $\sum\!\!\!\!\!\!\int_p = \sum_{n_p=-\infty}^{\infty} \int \frac{d^3p}{(2\pi)^3}$.

B. Two loop order diagrams

1. Two-point function

In TLA, we have to evaluate the following diagrams and express them in terms of thermal independent QFT diagrams with temperature function coefficients. The integral expressions of  ; in ITF and QFT are

$$\sum\!\!\!\!\!\!\int_{p_1,p_2} \frac{\lambda^2 T^2}{\varepsilon_{p1}^2 + \omega_{n_{p_1}}^2}\left[\frac{1}{\varepsilon_{p2}^2 + \omega_{n_{p_2}}^2}\right]^2 \tag{14}$$

and

$$\int \frac{\lambda^2}{\varepsilon_{p1}^2}\left[\frac{1}{\varepsilon_{p2}^2}\right]^2 \frac{d^4p_1}{(2\pi)^4}\frac{d^4p_2}{(2\pi)^4}, \tag{15}$$

respectively, with $\varepsilon_p^2 = p^2 + m^2$. We follow the same convention as shown in Sec. II A. As specified in Appendixes A-3 and A-4, after regularization ($\lambda \to g\mu^\epsilon, \frac{d^3p}{(2\pi)^3} \to \frac{d^{3-\epsilon}p}{(2\pi)^{3-\epsilon}}, \frac{d^4p}{(2\pi)^4} \to \frac{d^{4-\epsilon}p}{(2\pi)^{4-\epsilon}}, \epsilon \to 0$) we get the results

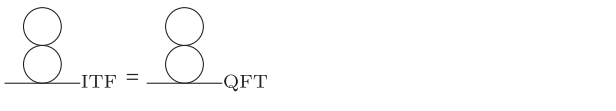

$$
\begin{aligned}
&- \left[g\mu^{\epsilon} \frac{S_0(m,T)}{4\pi} \right] \left[\text{QFT} \right] \\
&+ g\mu^{\epsilon} S_1(m,T) \frac{\partial}{\partial m^2} \left[\text{QFT} \right] \\
&+ (g\mu^{\epsilon})^2 \frac{S_1(m,T) S_0(m,T)}{4\pi}.
\end{aligned} \tag{16}
$$

The expressions for ⊖; in ITF and QFT are

$$
\sum\!\!\!\!\!\!\int_{p_1,p_2} \frac{1}{\varepsilon_{p_1}^2 + \omega_{n_{p_1}}^2} \frac{\lambda^2}{\varepsilon_{p_2}^2 + \omega_{n_{p_2}}^2} \frac{T^2}{\varepsilon_{p_1+p_2+q}^2 + \omega_{n_{p_1+p_2+q}}^2} \tag{17}
$$

and

$$
\int \frac{\lambda^2}{\varepsilon_{p_1}^2} \frac{1}{\varepsilon_{p_2}^2} \frac{1}{\varepsilon_{p_1+p_2+q}^2} \frac{d^4p_1}{(2\pi)^4} \frac{d^4p_2}{(2\pi)^4}, \tag{18}
$$

respectively. From the result of QFT [34,45,46] and corresponding ITF, after regularization ($\lambda \to g\mu^{\epsilon}$, $d^3p \to d^{3-\epsilon}p$, $d^4p \to d^{4-\epsilon}p$), we express the sunset/sunrise diagram at external momentum zero as

$$
\begin{aligned}
&+ \frac{S_1(m,T)}{2} \frac{g^2\mu^{\epsilon}}{(4\pi)^2} \left[\psi(1) + \ln\left(\frac{4\pi\mu^2}{m^2} \right) + \frac{2}{\epsilon} \right] \\
&+ \frac{S_1(m,T)}{2} \frac{g^2\mu^{\epsilon}}{(4\pi)^2} \left(2 - \frac{\pi}{\sqrt{3}} \right) + \frac{g^2m^2}{64\pi^4} Y(m,T) \\
&+ \mathcal{O}(\epsilon),
\end{aligned} \tag{19}
$$

where

$$
Y(m,T) = \int_0^{\infty} \int_0^{\infty} U(x)U(y)G(x,y)dxdy, \tag{20}
$$

$$
U(x) = \frac{\sinh(x)}{\exp\left(\beta m \cosh(x)\right) - 1}, \tag{21}
$$

$$
G(x,y) = \ln\left(\frac{1 + 2\cosh(x-y)}{1 + 2\cosh(x+y)} \frac{1 - 2\cosh(x+y)}{1 - 2\cosh(x-y)} \right), \tag{22}
$$

$$
S_N(m,T) = \frac{1}{\pi} \sum_{j=1}^{\infty} \left(\frac{m}{2\pi j\beta} \right)^N K_N(j\beta m). \tag{23}
$$

In these two cases, the remaining $g\mu^{\epsilon}$ will become $\lambda \approx g$ at $\epsilon \to 0$. Similarly in the case of finite terms, $(g\mu^{\epsilon})^2 = \lambda^2 \approx g^2$ as $\epsilon \to 0$. Detailed expansion and results are given in Appendixes A-3 and A-4.

2. Four-point function

This section also expresses the other relevant ϕ^4 four-point diagrams in TLA according to the same convention as Sec. II A. We have regularized results

$$
\begin{aligned}
&- 2g\mu^{\epsilon} W(k,n_k) \left[\text{QFT},k_0=\omega_{n_k} \right] \\
&- (g\mu^{\epsilon})^3 W^2(k,n_k),
\end{aligned} \tag{24}
$$

where

$$
-\lambda^3 \left(\sum\!\!\!\!\!\!\int_p \frac{T}{\varepsilon_{p-k}^2 + \omega_{n_{p-k}}^2} \frac{1}{\varepsilon_p^2 + \omega_{n_p}^2} \right)^2 \tag{25}
$$

and

$$
-\lambda^3 \left(\int \frac{1}{\varepsilon_{p-k}^2} \frac{1}{\varepsilon_p^2} \frac{d^4p}{(2\pi)^4} \right)^2 \tag{26}
$$

are corresponding nonregularized integral expressions for ITF and QFT. Here $[\omega_{n_k}, \vec{k}]$ denotes one of three momentum combinations $[\omega_{n_{k_1}} + \omega_{n_{k_2}}, \vec{k}_1 + \vec{k}_2]$, $[\omega_{n_{k_1}} + \omega_{n_{k_3}}, \vec{k}_1 + \vec{k}_3]$, and $[\omega_{n_{k_1}} + \omega_{n_{k_4}}, \vec{k}_1 + \vec{k}_4]$. Detailed expansion and derivation are given in Appendixes A-5 and A-6. Another required diagram and its ITF and QFT relations can be expressed as

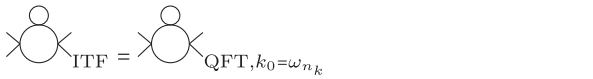

$$
\begin{aligned}
&+ \frac{g\mu^{\epsilon} S_1(m,T)}{2} \frac{\partial}{\partial m^2} \left[\text{QFT},k_0=\omega_{n_k} \right] \\
&- \frac{(g\mu^{\epsilon})^2}{2} \frac{\partial\, W(k,n_k)}{\partial m^2} \left[\text{QFT} \right] \\
&+ (g\mu^{\epsilon})^3 \frac{S_1(m,T)}{2} \frac{\partial}{\partial m^2} W(k,n_k).
\end{aligned} \tag{27}
$$

The integral expression of the above diagram is

$$
-\lambda^3 T^2 \sum\!\!\!\!\!\!\int_p \frac{1}{\varepsilon_{p-k}^2 + \omega_{n_p-n_k}^2} \frac{1}{(\varepsilon_p^2 + \omega_{n_p}^2)^2} \sum\!\!\!\!\!\!\int_q \frac{1}{\varepsilon_q^2 + \omega_{n_q}^2} \tag{28}
$$

and

$$
-\lambda^3 \int \frac{d^4p}{(2\pi)^4} \frac{1}{\varepsilon_{p-k}^2} \frac{1}{(\varepsilon_p^2)^2} \int \frac{d^4q}{(2\pi)^4} \frac{1}{\varepsilon_q^2} \tag{29}
$$

for ITF and nonthermal QFT, respectively. By defining operator $\mathcal{K}$ [34], which picks up the diverging terms from the corresponding graphs on which it has applied [i.e.,

$\mathcal{K}(\frac{A}{\epsilon^n}+B+c\epsilon)=\frac{A}{\epsilon^n}$], another complex diagram result can be summarized as

$$\mathcal{K}\left[\quad_{ITF}\right]=\mathcal{K}\left[\quad_{QFT,k_{0i}=\omega_{n_i}}\right]-g\mu^{\epsilon}W(k_i,n_{k_i})\mathcal{K}\left(\quad_{QFT}\right) \tag{30}$$

with

$$\int\frac{1}{\varepsilon_p^2}\frac{-\lambda^3}{\varepsilon^2_{k_1+k_2-p}}\frac{1}{\varepsilon_q^2}\frac{1}{\varepsilon^2_{p-q+k_3}}\frac{d^4p}{(2\pi)^4}\frac{d^4q}{(2\pi)^4} \tag{31}$$

and

$$\sum\!\!\!\!\!\!\int_{p,q}\frac{1}{\varepsilon_p^2+\omega^2_{n_p}}\frac{-\lambda^3T^2}{\varepsilon^2_{k_1+k_2-p}+\omega^2_{n_{k_1+k_2-p}}}\frac{1}{\varepsilon_q^2+\omega^2_{n_q}}\frac{1}{\varepsilon^2_{p-q+k_3}+\omega^2_{n_{p-q+k_3}}}. \tag{32}$$

These are the diagram's nonregularized integral expressions in QFT and ITF, respectively. The complete derivation of the above diagram is in Appendix A-7.

III. COUNTERTERMS AND MINIMAL SUBTRACTION SCHEME

Counterterm diagrams are those that make the vertex function finite when added with the vertex function. The previously derived diagrams in Sec. II contain terms that diverge for $\epsilon\to 0$. We redefine the proper vertex function to the divergence removed proper vertex function (FPVF). We use the MS scheme to deal with diverging terms. Here, operator $\mathcal{K}$ separates the diverging terms, i.e.,

$$\tilde{\Gamma}^{(n)}=\Gamma^{(n)}-\mathcal{K}(\Gamma^{(n)}). \tag{33}$$

By this definition

$$\tilde{\Gamma}^{(2)}=\Gamma^{(2)}-\mathcal{K}(\Gamma^{(2)}), \tag{34}$$

$$\tilde{\Gamma}^{(4)}=\Gamma^{(4)}-\mathcal{K}(\Gamma^{(4)}). \tag{35}$$

A. One loop calculation

The counterterms in one loop order are usually the pole term in diagrams with a negative sign.

1. Two-point function

We have to find the counterterm for first-order g, and we follow [34] as the reference text; then

$$\tilde{\Gamma}^{(2)}=(\quad)^{-1}_{\mathrm{ITF}}-\left\{\frac{1}{2}\quad_{\mathrm{ITF}}+\quad+\quad\right\}+\mathcal{O}(g^2), \tag{36}$$

where $\times$ represents the contribution of the mass counterterm, $\circ$ represents the field contribution, and $(\quad)$ under Euclidean momentum representation. In imaginary time formalism [39,44], the tadpole diagram's diverging term is the same as that of nonthermal QFT. The counterterm needed to cancel the tadpole divergence is proportional to m^2 and is

$$\begin{aligned}\times&=-m^2c^1_{m^2}=-\frac{1}{2}\mathcal{K}\left(\quad_{\mathrm{ITF}}\right)\\&\text{from Appendix A-1}\\&=-\frac{1}{2}\mathcal{K}\left(\quad_{\mathrm{QFT}}\right)\\&=-m^2\frac{g}{(4\pi)^2}\frac{1}{\epsilon},\end{aligned} \tag{37}$$

and the counterterm proportional to K^2 in first-order g is zero, so

$$-K^2c^1_{\phi}=\quad=0. \tag{38}$$

Thus the finite proper vertex function, which is finite at $\epsilon\to 0$,

$$\begin{aligned}\tilde{\Gamma}^{(2)}&=(\quad)^{-1}-\left(\frac{1}{2}\quad_{\mathrm{ITF}}-\frac{1}{2}\mathcal{K}\left(\quad_{\mathrm{ITF}}\right)\right)+\mathcal{O}(g^2)\\&=(\quad)^{-1}-\left(\frac{1}{2}\quad_{\mathrm{QFT}}-\frac{1}{2}\mathcal{K}\left(\quad_{\mathrm{QFT}}\right)\right)+\frac{g}{2}S_1(m,T)+\mathcal{O}(g^2).\end{aligned} \tag{39}$$

2. Four-point function

Similar to the two-point function case, the four-point finite proper vertex function is

$$\tilde{\Gamma}^{(4)}=-\left(\times+\frac{3}{2}\quad_{\mathrm{ITF}}+\quad_{\mathrm{ITF}}\right)+\mathcal{O}(g^3). \tag{40}$$

The counterterm is the pole term of the scattering diagram with a negative sign. In both ITF and QFT, the pole term is the same. Scattering diagrams in ITF and QFT differ by a finite thermal term:

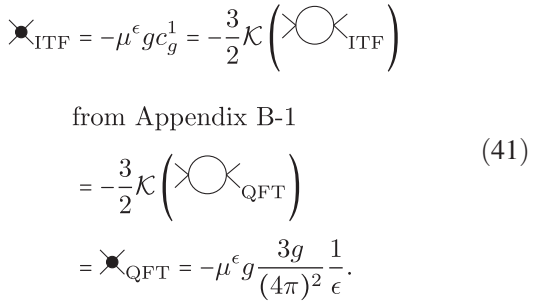

(41)

B. Two loop calculation

The redefinition of the proper vertex function in one loop order [Eqs. (36) and (40)] to make it finite causes more counterterm diagrams to emerge in the two loop order calculation.

1. Two-point function

The finite two-point function up to TLA for ITF is

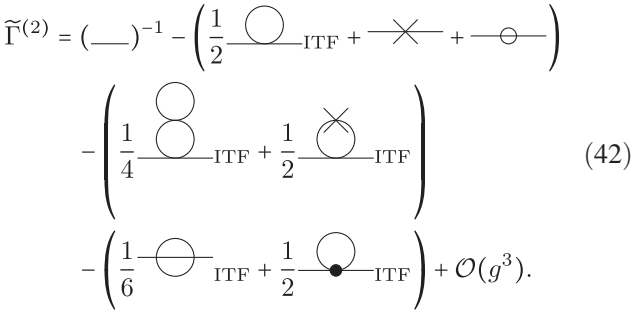

(42)

When compared to Eq. (2), the additional terms that appear here are the counterterm diagrams in two loop order to make the proper vertex function finite.

The pole term ($1/\epsilon^n$, $n > 0$) can have both thermal and nonthermal coefficients. Substituting $-m^2 c^1_{m^2}$ of Eq. (37) for $-g\mu^\epsilon$ in Eq. (9) the scattering diagram at $n_k, k = 0$ gives one of the counterdiagrams required. Appendix B-2 contains the detailed derivation:

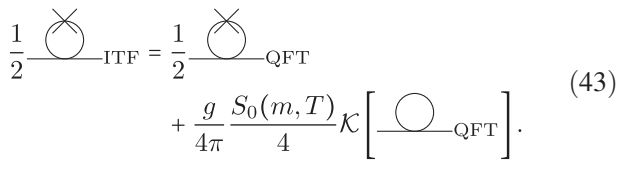

(43)

It is possible to express the counterterm diagram as the sum of similar diagrams in QFT with nonthermal coefficients and other diagrams with thermal coefficients, as shown above.

As given in Appendix B-3, if we replace $-\mu^\epsilon g$ in the tadpole of Eq. (8), in ITF by $-\mu^\epsilon g c^1_g$ of Eq. (41) we get

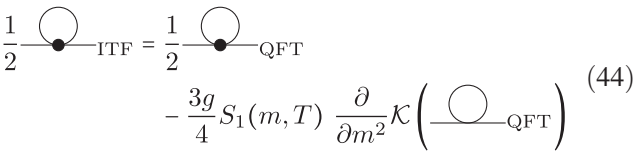

(44)

with

$$S_N(m,T) = \frac{1}{\pi}\sum_{j=1}^{\infty}\left(\frac{m}{2\pi j\beta}\right)^N K_N(j\beta m). \tag{45}$$

To find the remaining diverging terms in the vertex function, we write down the diverging terms of each diagram expressed in the two loop vertex function.

As stated in Appendix A-3 the diverging terms in the diagram in Eq. (16) expressed in terms of QFT poles with thermal and nonthermal coefficients are

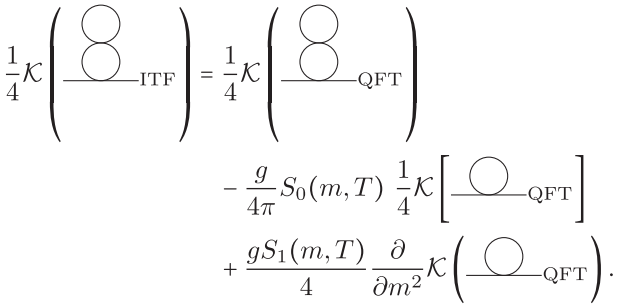

(46)

The diverging part of the sunset/sunrise diagram in the vertex function is

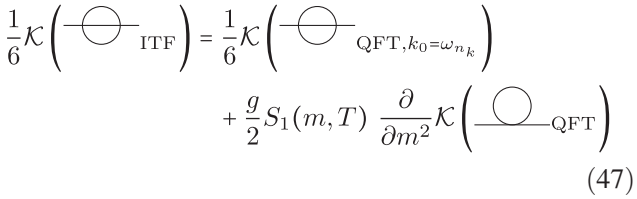

(47)

as described in Appendix A-4.

Interestingly ITF two-point functions total divergence is the same as that of QFT at $k_0 = \omega_{n_k}$, i.e.,

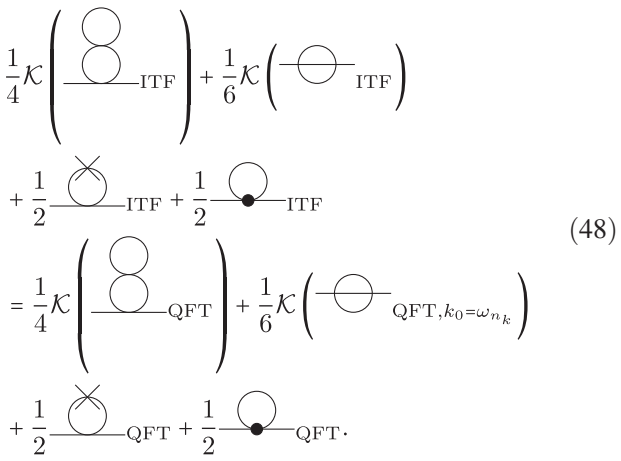

(48)

All other terms cancel with each other. Nevertheless, still, divergence exists in Eq. (48). c_{m^2} and c_ϕ absorb the remaining divergences. So the total contribution to counterterms c_{m^2} and c_ϕ up to g^2 in ITF is identical to that of QFT at $k_0 = \omega_{n_k}$:

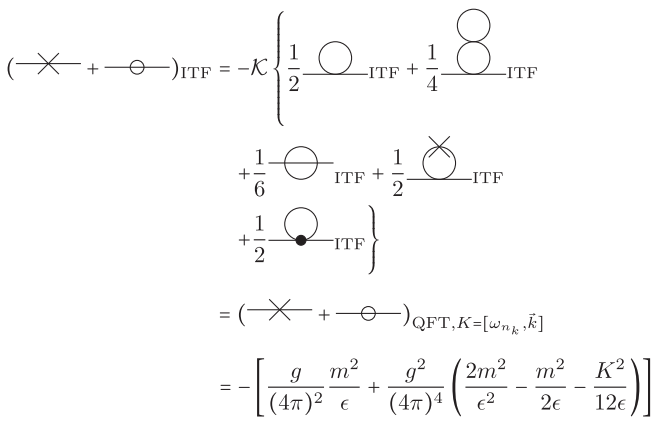

(49)

with $K^2 = \omega_{n_k}^2 + \vec{k}^2$.

That is, in ITF, if we follow the textbook procedure [34], the sum of counterterms is identical to that of QFT, with $k_0 = \omega_{n_k}$. If we extract the polynomial with coefficients m^2 and K^2, we get [34]

$$m^2(c^1_{m^2} + c^2_{m^2}) = m^2\left[\frac{g}{(4\pi)^2}\frac{1}{\epsilon} + \frac{g^2}{(4\pi)^4}\left(\frac{2}{\epsilon^2} - \frac{1}{2\epsilon}\right)\right]. \quad (50)$$

For field renormalization, we have to consider the term proportional to K^2, so

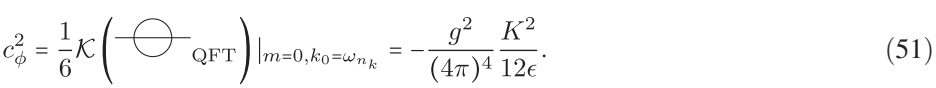

(51)

2. Four-point function

To proceed further, we have to remove the divergences of the four-point function using the renormalization procedure [34]. The result is the same as that of nonthermal QFT, i.e.,

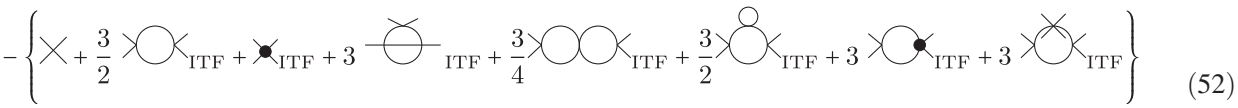

(52)

From Appendix A, one can verify the above results with complete derivation. Taking those results, we write from Appendix A-7

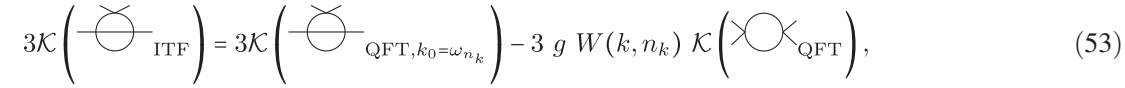

(53)

from Appendix A-5 as

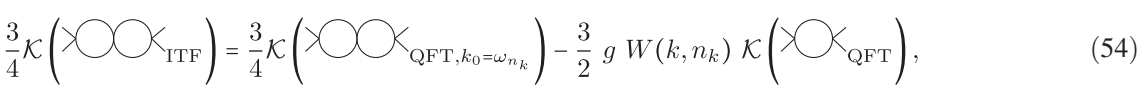

(54)

and from Appendix A-6 as

$$\frac{3}{2}\mathcal{K}\left(\text{ 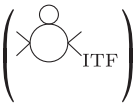 }_{\text{ITF}}\right) = \frac{3}{2}\mathcal{K}\left(\text{ 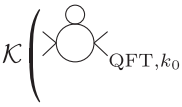 }_{\text{QFT},k_0=\omega_{n_k}}\right) - \frac{3g^2}{4}\frac{\partial\, W(k,n_k)}{\partial m^2}\,\mathcal{K}\left[\text{ 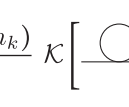 }_{\text{QFT}}\right]. \tag{55}$$

The counterterm derived for the four-point function from Appendix B-4 is

$$3\mathcal{K}\left(\text{ 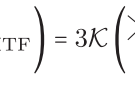 }_{\text{ITF}}\right) = 3\mathcal{K}\left(\text{ 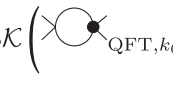 }_{\text{QFT},k_0=\omega_{n_k}}\right) + \frac{9}{2}\, g\, W(k,n_k)\,\mathcal{K}\left(\text{ 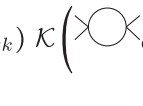 }_{\text{QFT}}\right); \tag{56}$$

the other counterterm for the four-point function from Appendix B-5 is

$$3\mathcal{K}\left(\text{ 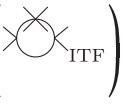 }_{\text{ITF}}\right) = 3\mathcal{K}\left(\text{  }_{\text{QFT},k_0=\omega_{n_k}}\right) + \frac{3}{4}g^2\left(\frac{\partial W(k,n_k)}{\partial m^2}\right)\mathcal{K}\left[\text{ 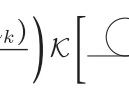 }_{\text{QFT}}\right]. \tag{57}$$

Adding Eqs. (53)–(57), we get

$$\left\{3\mathcal{K}\left(\text{ 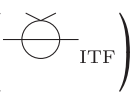 }_{\text{ITF}}\right) + \frac{3}{4}\mathcal{K}\left(\text{  }_{\text{ITF}}\right) + \frac{3}{2}\mathcal{K}\left(\text{ 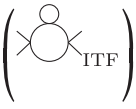 }_{\text{ITF}}\right) + 3\mathcal{K}\left(\text{  }_{\text{ITF}}\right) + 3\mathcal{K}\left(\text{  }_{\text{ITF}}\right)\right\} \tag{58}$$

$$= \left\{3\mathcal{K}\left(\text{ 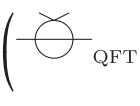 }_{\text{QFT}}\right) + \frac{3}{4}\mathcal{K}\left(\text{ 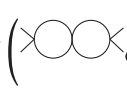 }_{\text{QFT}}\right) + \frac{3}{2}\mathcal{K}\left(\text{ 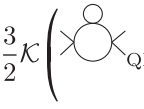 }_{\text{QFT}}\right) + 3\mathcal{K}\left(\text{ 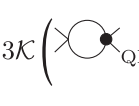 }_{\text{QFT}}\right) + 3\mathcal{K}\left(\text{  }_{\text{QFT}}\right)\right\}|_{k_0=\omega_{n_k}}. \tag{59}$$

IV. RENORMALIZATION CONSTANTS

Therefore, we get the renormalization constants as

$$\begin{aligned} Z_g(g,\epsilon^{-1}) &= 1 + \frac{1}{g\mu^\epsilon}\left\{\frac{3}{2}\mathcal{K}\left(\text{ 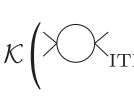 }_{\text{ITF}}\right) + 3\mathcal{K}\left(\text{ 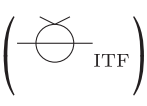 }_{\text{ITF}}\right) + \frac{3}{4}\mathcal{K}\left(\text{ 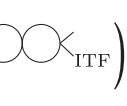 }_{\text{ITF}}\right) + \frac{3}{2}\mathcal{K}\left(\text{ 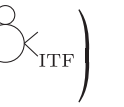 }_{\text{ITF}}\right)\right. \\ &\qquad \left. + 3\mathcal{K}\left(\text{ 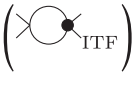 }_{\text{ITF}}\right) + 3\mathcal{K}\left(\text{ 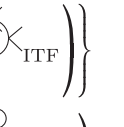 }_{\text{ITF}}\right)\right\} \\ &= 1 + \frac{1}{g\mu^\epsilon}\left\{\frac{3}{2}\mathcal{K}\left(\text{ 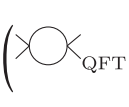 }_{\text{QFT}}\right) + 3\mathcal{K}\left(\text{  }_{\text{QFT}}\right) + \frac{3}{4}\mathcal{K}\left(\text{ 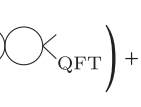 }_{\text{QFT}}\right) + \frac{3}{2}\mathcal{K}\left(\text{  }_{\text{QFT}}\right)\right. \\ &\qquad \left. + 3\mathcal{K}\left(\text{ 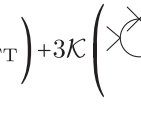 }_{\text{QFT}}\right) + 3\mathcal{K}\left(\text{ 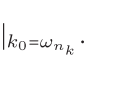 }_{\text{QFT}}\right)\right\}|_{k_0=\omega_{n_k}}. \end{aligned} \tag{60}$$

So from the standard result of QFT [34] under SMC,

$$Z_g(g,\epsilon^{-1}) = 1 + \frac{g}{(4\pi)^2}\frac{3}{\epsilon} + \frac{g^2}{(4\pi)^4}\left(\frac{9}{\epsilon^2} - \frac{3}{\epsilon}\right). \tag{61}$$

Similarly, from Eqs. (48) and (50), Appendix A-1, and Secs. III B and III A 1,

$$Z_{m^2} = 1 + \frac{1}{m^2}\left\{\frac{1}{2}\mathcal{K}\left(\text{ITF}\right) + \frac{1}{4}\mathcal{K}\left(\text{ITF}\right) + \frac{1}{6}\mathcal{K}\left(\text{ITF},K^2=0\right) + \frac{1}{2}\mathcal{K}\left(\text{ITF}\right) + \frac{1}{2}\mathcal{K}\left(\text{ITF}\right)\right\}$$
$$= 1 + \frac{1}{m^2}\left\{\frac{1}{2}\mathcal{K}\left(\text{QFT}\right) + \frac{1}{4}\mathcal{K}\left(\text{QFT}\right) + \frac{1}{6}\mathcal{K}\left(\text{QFT},K^2=0\right) + \frac{1}{2}\mathcal{K}\left(\text{QFT}\right) + \frac{1}{2}\mathcal{K}\left(\text{QFT}\right)\right\}, \tag{62}$$

$$Z_{m^2}(g,\epsilon^{-1}) = 1 + \frac{g}{(4\pi)^2}\frac{1}{\epsilon} + \frac{g^2}{(4\pi)^4}\left(\frac{2}{\epsilon^2} - \frac{1}{2\epsilon}\right). \tag{63}$$

From Sec. III A 1 and Eq. (51), we get

$$Z_\phi = 1 + \frac{1}{K^2}\frac{1}{6}\mathcal{K}\left(QFT\right)|_{m^2=0,k_0=\omega_{n_k}}$$
$$= 1 + c_\phi \tag{64}$$
$$= 1 - \frac{g^2}{(4\pi)^4}\frac{1}{12\epsilon}$$

The above results show that for two- and four-point functions at TLA, the values of Z_ϕ, Z_g, and Z_{m^2} for ITF are the same as for nonthermal ϕ^4 theory [34]. So we demand that the RGE for QFT must also be true for ITF.

V. RENORMALIZATION GROUP EQUATION IN TWO LOOP ORDER TWO-POINT FUNCTION

The previous results show that no Z_ϕ, Z_g, or Z_{m^2} is explicitly temperature dependent, and they agree with the nonthermal field theory. However, a nonexplicit reliance may exist via the coupling constant g as $g(\mu(T))$. Furthermore, we use RGE for TLA to see if such relationships are possible; i.e., we demand Eqs. (66)–(70) to be true for TLA under SMC. Here the RGE is explicitly temperature independent, but the vertex function in ITF is temperature dependent.

$$\frac{d}{d(\ln\mu)}\tilde{\Gamma}^{(n)}(m,g,T,\mu) = \left[\mu\frac{\partial}{\partial\mu} + \beta(g)\frac{\partial}{\partial g} - n\gamma(g) + \gamma_m m\frac{\partial}{\partial m}\right]\tilde{\Gamma}^{(n)}(m,g,T,\mu) \approx_{\text{TLA}} 0, \tag{65}$$

$$\left[\mu\frac{\partial}{\partial\mu} + \beta(g)\frac{\partial}{\partial g} - 2\gamma(g) + \gamma_m m\frac{\partial}{\partial m}\right]\tilde{\Gamma}^{(2)}_{\text{ITF}}(m,g,T,\mu) \approx_{\text{TLA}} 0, \tag{66}$$

$$\left[\mu\frac{\partial}{\partial\mu} + \beta(g)\frac{\partial}{\partial g} - 2\gamma(g) + \gamma_m m\frac{\partial}{\partial m}\right]\tilde{\Gamma}^{(2)}_{\text{QFT}}(m,g,T,\mu) \approx_{\text{TLA}} 0, \tag{67}$$

$$\frac{dg}{d\ln(\mu)} = \beta(g) \approx \beta_2 g^2 + \beta_3 g^3, \tag{68}$$

$$\frac{d\ln(m(\mu))}{d\ln(\mu)} = \gamma_m(g) \approx \gamma_{m_1} g + \gamma_{m_2} g^2, \tag{69}$$

$$\gamma(g) \approx \gamma_2 g^2. \tag{70}$$

In the previous section, we expressed ITF diagrams as the sum of corresponding QFT diagrams with subdiagrams having thermal coefficients. Therefore we can write the FPVF in ITF as the sum of FPVF of QFT with some subdiagrams having thermal coefficients under SMC.

At external momentum zero, we can write

$$\tilde{\Gamma}^{(2)\mathrm{ITF}}_{\mathrm{finite},K=0} = \tilde{\Gamma}^{(2)\mathrm{QFT}}_{\mathrm{finite},K=0} + \Gamma^{\mathrm{diff}}, \tag{71}$$

where $\tilde{\Gamma}^{(2)}_{\mathrm{finite}} = \Gamma^{(2)} - \mathcal{K}(\Gamma^{(2)})$.

Thus any RGE that is valid for both ITF and QFT will also be true for their differences $(\tilde{\Gamma}^{(2)}_{\mathrm{ITF}} - \tilde{\Gamma}^{(2)}_{\mathrm{QFT}})$. Then Eqs. (66) and (67) lead to

$$\left\{\frac{\partial}{\partial \ln(\mu)} + \beta(g)\frac{\partial}{\partial g} - 2\gamma(g) + \gamma_m \frac{\partial}{\partial \ln(m)}\right\}\Gamma^{\mathrm{diff}} = 0. \tag{72}$$

From the previous section, it is clear that the individual Feynman diagram evaluated in ITF and QFT at $k_0 = \omega_{n_k}$ is different. Still, the two-point and four-point vertex divergences are of the same form. Thus the renormalization constants $(Z_{m^2}, Z_g, \ldots, c_{m^2}, c_g)$ are in the same structure. Therefore we can use the results of nonthermal ϕ^4 theory for finite functions $\beta(g)$, $\gamma(g)$, and $\gamma_m(g)$ from [34] for ITF also.

At $K \neq 0$, the functions are

$$\begin{aligned}
\gamma(g) &= \frac{g^2}{(4\pi)^4}\frac{1}{12} = \gamma_2 g^2, \\
\gamma_m(g) &= \frac{1}{2}\frac{g}{(4\pi)^2} - \frac{5}{12}\frac{g^2}{(4\pi)^4} = g\gamma_{m1} + g^2\gamma_{m2}, \\
\beta(g) &= -\epsilon g + \frac{3g^2}{(4\pi)^2} - \frac{17g^3}{3(4\pi)^4} = g\beta_1 + g^2\beta_2 + g^3\beta_3.
\end{aligned} \tag{73}$$

When $K \to 0$, $\epsilon \to 0$, as shown in Appendix C, the functions change to

$$\begin{aligned}
\gamma(g) &= \gamma_2 g^2 = 0, \\
\gamma_m(g) &= \frac{1}{2}\frac{g}{(4\pi)^2} - \frac{1}{2}\frac{g^2}{(4\pi)^4} = g\gamma_{m1} + g^2\gamma_{m2}, \\
\beta(g) &= \frac{3g^2}{(4\pi)^2} - \frac{6g^3}{(4\pi)^4} = g^2\beta_2 + g^3\beta_3.
\end{aligned} \tag{74}$$

The general form of the two-point FPVF at TLA is

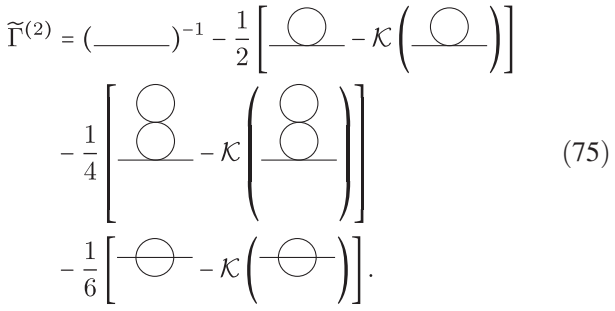

In order to simplify these equations, let us define an operator

$$\begin{aligned}
\Delta(\mathbb{A}) = {} & \mathbb{A}_{\mathrm{ITF}}|_{k,\omega_{n_k}=0} - \mathcal{K}(\mathbb{A}_{\mathrm{ITF}})|_{k,\omega_{n_k}=0} \\
& - \mathbb{A}_{\mathrm{QFT}}|_{k_0,k=0} + \mathcal{K}(\mathbb{A}_{\mathrm{QFT}})|_{k_0,k=0},
\end{aligned} \tag{76}$$

where $\mathbb{A}$ represents the appropriate diagram.

Since we defined $\Gamma^{\mathrm{diff}}_{n_k,\vec{k}=0} = \Gamma^{(2)\mathrm{ITF}}|_{n_k,k=0} - \Gamma^{(2)\mathrm{QFT}}|_{k_0,k=0}$, we get

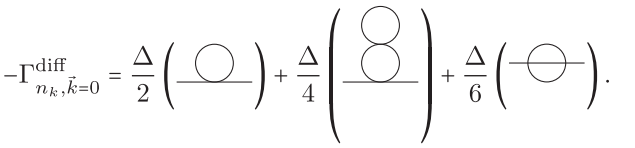

(77)

From Appendix A-1, we get

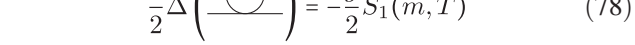

(78)

From Appendix A-3, we get

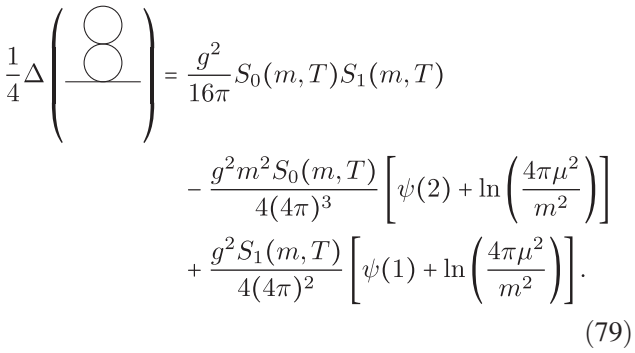

(79)

From Appendix A-4, we get

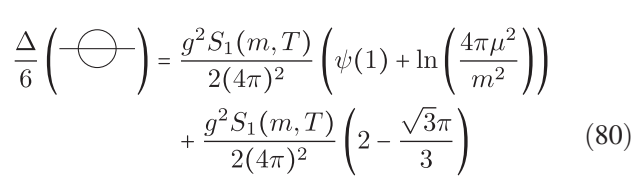

(80)

with

$$Y(m,T) = \int_0^\infty \int_0^\infty U(x)U(y)G(x,y)dxdy, \tag{81}$$

$$U(x) = \frac{\sinh(x)}{\exp(\beta m \cosh(x)) - 1}, \tag{82}$$

$$G(x,y) = \ln\left(\frac{1+2\cosh(x-y)}{1+2\cosh(x+y)}\frac{1-2\cosh(x+y)}{1-2\cosh(x-y)}\right). \tag{83}$$

Therefore by combining the above results, we get

$$\Gamma^{\text{diff}}_{n_k,\vec{k}=0} = \frac{g}{2}S_1(m,T) - \frac{3g^2}{4}\frac{S_1(m,T)}{(4\pi)^2}\left[\psi(1)+\ln\left(\frac{4\pi\mu^2}{m^2}\right)\right] - \frac{g^2}{4(4\pi)}S_0(m,T)S_1(m,T) + \frac{g^2m^2}{4(4\pi)^3}S_0(m,T)\left[\psi(2)+\ln\left(\frac{4\pi\mu^2}{m^2}\right)\right] - \frac{g^2m^2}{64\pi^4}Y(m,T) - \frac{g^2}{32\pi^2}S_1(m,T)\left[2-\frac{\pi}{\sqrt{3}}\right]. \tag{84}$$

Thus combining Eqs. (84) and (72) and expanding it as a polynomial in g looks like a polynomial of order four. However, as shown in Appendix D, the coefficients of g^2, g, and g^0 are zero and lead to first-degree polynomials. When we rearrange the linear equation in g, we get

$$g(m,T,\mu) = \frac{A(m,T)\ln(\mu)+B(m,T)}{C(m,T)\ln(\mu)+D(m,T)} \tag{85}$$

with

$$A = [-\gamma_{m1}V_{2,\ln m} - 2\beta_2 V_2(m,T)], \tag{86}$$

$$C = [2(\beta_3-\gamma_2)V_2 + \gamma_{m2}V_{2,\ln m}], \tag{87}$$

$$B = (2\gamma_2-\beta_3)T_1 - 2\beta_2 V_1(m,T) - \gamma_{m1}V_{1,\ln m} - \gamma_{m2}T_{1,\ln m}, \tag{88}$$

$$D = 2(\beta_3-\gamma_2)V_1 + \gamma_{m2}V_{1,\ln m}, \tag{89}$$

$$T_1 = \frac{1}{2}S_1(m,T), \tag{90}$$

$$T_{1,\ln m} = -\frac{m^2}{4\pi}S_0(m,T), \tag{91}$$

$$V_1(m,T) = \frac{m^2}{4(4\pi)^3}S_0(m,T)\left[\psi(2)+\ln\left(\frac{4\pi}{m^2}\right)\right] - \frac{3}{4}\frac{S_1(m,T)}{(4\pi)^2}\left[\psi(1)+\ln\left(\frac{4\pi}{m^2}\right)\right] - \frac{1}{4(4\pi)}S_0(m,T)S_1(m,T) - \frac{m^2}{64\pi^4}Y(m,T) - \frac{S_1(m,T)}{32\pi^2}\left[2-\frac{\sqrt{3}\pi}{3}\right], \tag{92}$$

$$V_2(m,T) = \left(\frac{m^2}{2(4\pi)^3}S_0(m,T) - \frac{3S_1(m,T)}{2(4\pi)^2}\right), \tag{93}$$

$$V_{2,\ln m} = \frac{4m^2S_0(m,T)}{(4\pi)^3} - \frac{m^4S_{-1}(m,T)}{(4\pi)^4}, \tag{94}$$

$$V_{1,\ln m} = \frac{2m^2}{(4\pi)^3}S_0(m,T)\left[\psi(1)+\ln\left(\frac{4\pi}{m^2}\right)\right] - \frac{m^4}{2(4\pi)^4}S_{-1}(m,T)\left[\psi(2)+\ln\left(\frac{4\pi}{m^2}\right)\right] + \frac{3}{2}\frac{S_1(m,T)}{(4\pi)^2} + \frac{m^2S_0^2(m,T)}{2(4\pi)^2} + \frac{m^2}{2(4\pi)^2}S_1(m,T)S_{-1}(m,T) + \frac{m^2S_0(m,T)}{(4\pi)^3}\left[2-\frac{\sqrt{3}\pi}{3}\right] - \frac{m^2}{32\pi^4}Y(m,T) - \frac{m^4}{32\pi^4}\frac{\partial Y(m,T)}{\partial m^2}. \tag{95}$$

The other trivial value of g that satisfies these equations is zero, so we do not care about those solutions. Instead, choosing another physically possible solution [as in Eq. (85)] leads to a thermal-dependent coupling constant. If we combine with a beta coupling constant relation such as

$$\frac{dg(\mu)}{d\ln(\mu)} = \beta_2 g^2 + \beta_3 g^3, \tag{96}$$

it gives rise to the result

$$\ln(\mu) = \int^g \frac{1}{\beta_2 t^2+\beta_3 t^3}dt = -\frac{1}{\beta_2 g} + \frac{\beta_3}{\beta_2^2}\ln\left(\beta_3+\frac{\beta_2}{g}\right) + \ln\mu_0. \tag{97}$$

Similarly, the corresponding running mass coupling relation is

$$\frac{d\ln(m)}{d\ln(\mu)} = \gamma_m(g). \tag{98}$$

When combined with Eq. (96), it results in

$$\frac{\partial\ln(m)}{\partial g}\frac{dg}{d\ln(\mu)} = \gamma_m(g) \tag{99}$$

$$\Rightarrow \frac{\partial\ln(m)}{\partial g} = \frac{\gamma_m(g)}{\beta(g)} = \frac{\gamma_{m1}+\gamma_{m2}g}{\beta_2 g+\beta_3 g^2},$$

$$\ln\left(\frac{m}{m_0}\right) = \chi_2 + \frac{\gamma_{m1}}{\beta_2}\ln(g) + \left(\frac{\gamma_{m2}}{\beta_3}-\frac{\gamma_{m1}}{\beta_2}\right)\ln(\beta_3 g+\beta_2), \tag{100}$$

where $\ln\mu_0$, m_0, and χ_2 are the respective integration constants.

Solving Eqs. (97), (100), and (85) simultaneously, we get the temperature-dependent running mass and coupling constant.

Combining the above results with the quasiparticle model of Bannur [5–7], we get expressions for energy density and pressure as

$$\varepsilon(T) = g_f \frac{m^4}{2\pi^2} \sum_{n=1}^{\infty} \left[\frac{3K_2\left(\frac{nm}{T}\right)}{\left(\frac{nm}{T}\right)^2} + \frac{K_1\left(\frac{nm}{T}\right)}{\frac{nm}{T}} \right] \tag{101}$$

$$= g_f \frac{m^4}{16\pi^2} \sum_{n=1}^{\infty} \left[K_4\left(\frac{nm}{T}\right) - K_0\left(\frac{nm}{T}\right) \right] \tag{102}$$

and

$$\frac{P}{T} - \frac{P_0}{T_0} = \int_{T_0}^{T} \frac{\varepsilon(m(T), T)}{T^2} dT. \tag{103}$$

VI. RESULTS AND DISCUSSION

We have derived an equation relating running mass, mass scale, coupling, and temperature, i.e., Eq. (85). Similarly, we have the equation connecting running coupling with mass scale known as the beta function equation as in Eq. (97). Furthermore, we have an equation connecting running mass and coupling as in Eq. (100). Solving Eqs. (85), (97), and (100) for each temperature value will give us the results as shown in the figures. If one wishes to keep the μ independent from this set of equations, then as pointed out in [34], one can redefine it as $\mu \to \sigma\mu$. In that case, our above expressions will be a particular case of $\sigma = 1$. One will have to rewrite all equations of RGE concerning these changes, and a new differential equation between σ and μ will appear, as shown in [34].

We plot the main results in Figs. 1–4, with varying integration constants. Two loop coupling constant results and two loop running mass results are shown in Figs. 1 and 2, respectively. It is evident from Fig. 2 that as temperature goes to infinity, the running mass per temperature goes to zero. To understand the nature of pressure proposed by the model, we plot pressure against temperature with different values of T_0, P_0 in Fig. 3. These results show similar trends, i.e., $\beta \to 0$; i.e., $T \to \infty$ pressure reaches the ideal limit $P_{\mathrm{SB}} = P_{\mathrm{ideal}} = \frac{\pi^2}{90}T^4$, irrespective of the initial value. P_{SB} is Stefan Boltzmann's limit of pressure. In Fig. 4, with a given $\ln\mu_0$ and χ_2, at high temperatures, the ratio μ/μ_0 goes to a constant value. The same trend can be seen in Fig. 1, i.e., going to a constant value at a high-temperature limit. Fitting with lattice data can be used to find appropriate integration constants μ_0 and χ_2. When $T \to 0$, as per

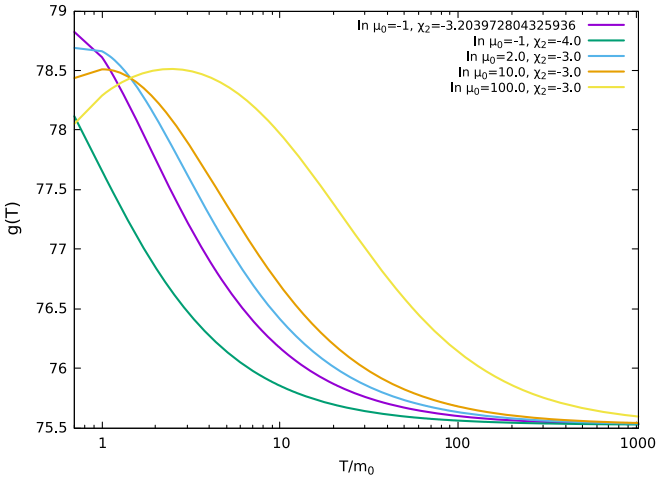

FIG. 1. Two loop coupling constant results. g against T/m_0 plotted with varying values of integration constants $\ln\mu_0$ and χ_2 with $m_0 \approx 1$.

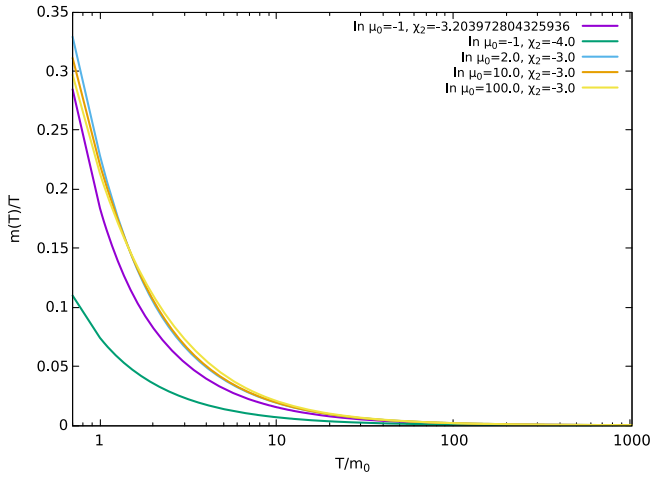

FIG. 2. Two loop running mass results. The difference between the curves is due to the different integration constants, as shown in the figure.

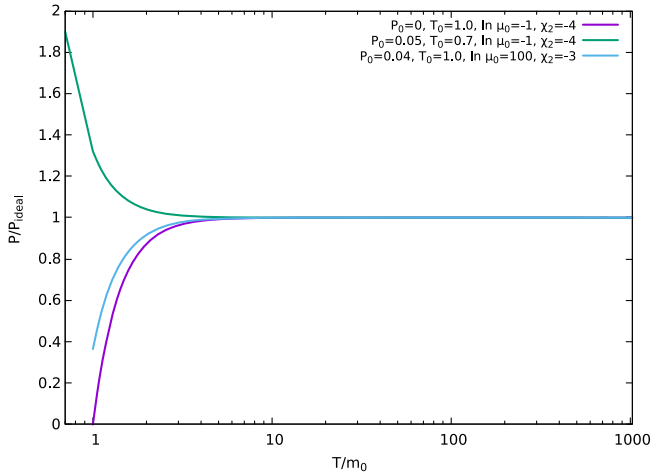

FIG. 3. Pressure scaled by $\frac{\pi^2}{90}T^4$ against T/m_0, with varying values of $T_0, P_0, \ln\mu_0, \chi_2$.

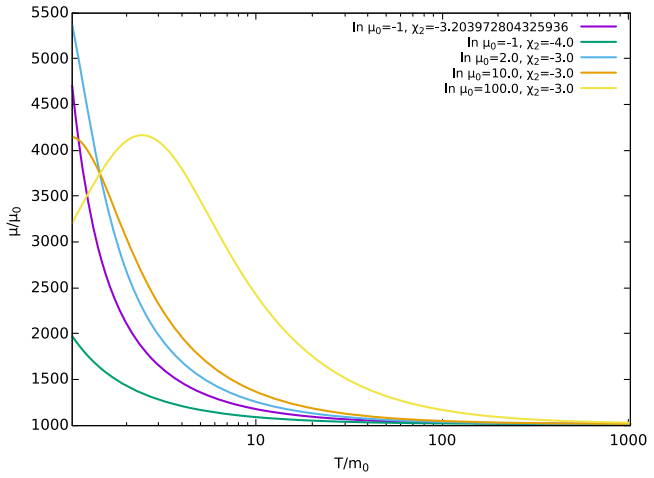

FIG. 4. $\frac{\mu}{\mu_0}$ plotted against T/m_0 with varying integration constants $\ln(\mu_0)$ and χ_2 with $m_0 \approx 1$.

Appendix D-1, $g \approx -(\gamma_{m1}/\gamma_{m2})$. As a result, at $T \approx 0$, $\ln(\mu/\mu_0)$ becomes a complex number. However, one can make the μ a real number by choosing μ_0, a negative number/complex number/complex function that can cancel the complex factor appearing on the right-hand side Eq. (97). The same holds for running mass. So by choosing the appropriate integration constants/functions at the zero temperature limit, one can still make the mass scale and running mass real or complex. These integral constants used in our model make it flexible. However, the best way to determine the value of integration constants will be to fit the actual data with the corresponding function once it becomes available. In our model rather than selecting the mass scale ourselves, we set the mass scale μ to be a parameter that obeys RGE. The temperature dependence came naturally.

The quasiparticle model [5–7] derives energy density from standard statistical mechanics at relativistic Bose-Einstein distribution. The pressure Eq. (103) has the property that at $T \to T_0$, the integral part of the equation becomes zero. Hence, the pressure converges to the P_0 value. From Appendix D-2, it is clear that as $T \to 0$, energy density $\varepsilon(T) \to 0$ and $\frac{\varepsilon(T)}{T^2} \to 0$.

VII. CONCLUSION

We conclude that the renormalization constants in imaginary time formalism with one and two loop approximations are identical to those in nonthermal QFT. In our new approach, by applying RGE on thermal and nonthermal vertex functions simultaneously, we derived the coupling constant and corresponding running mass at zero momentum limits, where self-energy is analytic [36]. The running mass and coupling constant with temperature dependence with varying integration constants are plotted in figures for massive ϕ^4 field theory. Combining these results with the quasiparticle model of Bannur [5–7] [Eqs. (101) and (103)] and by choosing different values for P_0 and T_0, we have evaluated the pressure for the temperature-dependent running mass. At higher temperatures, we observe pressure reaching its ideal limit $\frac{\pi^2}{90}T^4$ irrespective of its initial value of P_0/T_0. Our model is flexible in such a way that once the experimental data or lattice data are available for some range, we will be able to tweak the integration constants in our model and compare. It will be interesting to know the results when we extend this model to QCD in the future.

ACKNOWLEDGMENTS

One of the authors (K. A.) wishes to express gratitude to the Kerala State Council For Science, Technology and Environment for supporting the research by awarding KSCSTE Research Fellowship.

APPENDIX A: INTEGRAL EQUATIONS ITF TO NONTHERMAL QFT CONNECTIONS

Here we derive the necessary diagrams for the calculation. Also, we used approximations $\lambda = g\mu^\epsilon$ on regularization, especially at the final stage. We used an operator $\mathcal{K}$, which picks up the diverging terms from the corresponding graphs it applied. i.e., $\mathcal{K}(\frac{A}{\epsilon^n} + B + c\epsilon) = \frac{A}{\epsilon^n}$.

1. Diagram one loop A

We can write

$$\left[\{-\lambda\}\text{---}\bigcirc\text{---}_{\mathrm{ITF}}\right] = -\lambda T \sum\!\!\!\!\!\!\int \frac{1}{(2\pi n T)^2 + p^2 + m^2}$$
$$= -\lambda \int T \sum_{n=-\infty}^{\infty} \frac{1}{\omega_n^2 + \varepsilon_p^2} \frac{d^3p}{(2\pi)^3}$$
$$= -\lambda \int \frac{1}{P^2 + m^2} \frac{d^4P}{(2\pi)^4} - \lambda S_1(m,T)$$
$$= \left[\{-\lambda\}\text{---}\bigcirc\text{---}_{\mathrm{QFT}}\right] - \lambda S_1(m,T), \tag{A1}$$

where

$$S_1(m,T) = \int \frac{n_B(\beta\varepsilon_p)}{\varepsilon_p} \frac{d^3p}{(2\pi)^3} = \frac{1}{\pi} \sum_{n=1}^{\infty} \left(\frac{m}{2\pi n\beta}\right) K_1(n\beta m) \tag{A2}$$

with $K(n,x)$ is the modified Bessel function of the second kind and $n_B(x) = (\exp(x) - 1)^{-1}$.

The braces $\{\lambda\}$ serve as labels rather than a multiplication factor. If we proceed with dimensional regularization, then the Feynman diagram with substitution $\lambda = g\mu^\epsilon$ becomes

$$\left[\{-g\mu^{\epsilon}\}\text{---}\bigcirc\text{---}_{\mathrm{ITF}}\right] = \frac{m^2 g}{(4\pi)^2}\left[\frac{2}{\epsilon} + \psi(2) + \ln\left(\frac{4\pi\mu^2}{m^2}\right)\right] + \mathcal{O}(\epsilon) - g\mu^{\epsilon} S_1(m,T), \tag{A3}$$

where we used standard results [34],

$$\left[\{-g\mu^{\epsilon}\}\text{---}\bigcirc\text{---}_{\mathrm{QFT}}\right] = \frac{m^2 g}{(4\pi)^2}\left[\frac{2}{\epsilon} + \psi(2) + \ln\left(\frac{4\pi\mu^2}{m^2}\right)\right] + \mathcal{O}(\epsilon). \tag{A4}$$

Equation (A3) can be verified using a similar integral result [40,46]. The main difference is that we have defined

$$\lambda \sum\!\!\!\!\!\!\int f(p) = g\mu^{\epsilon} \sum_{n_p=-\infty}^{\infty} \int f(p) \frac{d^{N-\epsilon}p}{(2\pi)^{N-\epsilon}} \tag{A5}$$

while [40,46] defined it as

$$g^2 \sum\!\!\!\!\!\!\int_{\bar{M}S} f(p) = g^2 \left(\frac{e^{\gamma}\mu^2}{4\pi}\right)^{\epsilon} \sum_{n_p=-\infty}^{\infty} \int f(p) \frac{d^{N-2\epsilon}p}{(2\pi)^{N-2\epsilon}}. \tag{A6}$$

2. Diagram one loop B

The integration part of $2 \to 2$ scattering diagram without λ is

$$\int \frac{d^3p}{(2\pi)^3} T \sum_{n_p=-\infty}^{\infty} \frac{1}{\omega_{n_p}^2 + \varepsilon_p^2} \frac{1}{\omega_{n_p-n_r}^2 + \varepsilon_{p-r}^2} = \int \frac{1}{P^2+m^2} \frac{1}{(P-R)^2+m^2} \frac{d^4P}{(2\pi)^4} + \sum_{\sigma,\sigma_1=\pm 1} \int \frac{n_B(\beta\varepsilon_p)}{2\varepsilon_p\varepsilon_{p+r}} \frac{1}{\sigma_1\varepsilon_p + \varepsilon_{p+r} + i\sigma\omega_{n_r}} \frac{d^3p}{(2\pi)^3}. \tag{A7}$$

Corresponding diagrammatic expression is

$$\{(g\mu^{\epsilon})^2\}\text{><}\bigcirc\text{><}_{ITF} = \{(g\mu^{\epsilon})^2\}\text{><}\bigcirc\text{><}_{QFT,R_0=\omega_{n_r}} + (g\mu^{\epsilon})^2 W(r,n_r) \tag{A8}$$

with

$$W(r,n_r) = \int \frac{d^3p}{(2\pi)^3} \frac{2n_B(\beta\varepsilon_p)}{\varepsilon_p} \frac{r^2 + 2pr\cos\theta + \omega_{n_r}^2}{(r^2 + 2pr\cos\theta + \omega_{n_r}^2)^2 + 4\varepsilon_p^2\omega_{n_r}^2}. \tag{A9}$$

Applying dimensional regularization ($\lambda = g\mu^{\epsilon}$) and using the result from the standard textbook [34], we can write

$$\{g^2\mu^{\epsilon}\}\text{><}\bigcirc\text{><}_{ITF} = \frac{g^2\mu^{\epsilon}}{(4\pi)^2}\left(\frac{2}{\epsilon} + \psi(1) + \int_0^1 dx \ln\left[\frac{4\pi\mu^2}{R^2x(1-x)+m^2}\right]|_{R_0=\omega_{n_r}} + \mathcal{O}(\epsilon)\right) + g^2\mu^{2\epsilon} W(r,n_r) \tag{A10}$$

with $R = [\omega_{n_r}, r]$.

3. Diagram two loop C

The ITF and QFT relations for the diagram mentioned in Eq. (16) can be derived as

$$\{\lambda^2\}\,\text{(two-loop C)}_{\text{ITF}} = \int \lambda^2 T^2 \sum_{n_{p1}=-\infty}^{\infty} \sum_{n_{p2}=-\infty}^{\infty} \frac{1}{\omega_{n_{p1}}^2 + \varepsilon_{p1}^2} \left[\frac{1}{\omega_{n_{p2}}^2 + \varepsilon_{p2}^2}\right]^2 \frac{d^3p_1}{(2\pi)^3} \frac{d^3p_2}{(2\pi)^3}$$
$$= -\lambda T \int \sum_{n_{p1}=-\infty}^{\infty} \frac{1}{\omega_{n_{p1}}^2 + \varepsilon_{p1}^2} \frac{d^3p_1}{(2\pi)^3} \times -\frac{\partial}{\partial m^2} \left[-\lambda T \int \sum_{n_{p1}=-\infty}^{\infty} \frac{1}{\omega_{n_{p1}}^2 + \varepsilon_{p1}^2} \frac{d^3p_1}{(2\pi)^3}\right]. \tag{A11}$$

Using the results from [34] and from Eq. (A1) we can write

$$\text{(two-loop C)}_{\text{ITF}} = \text{(two-loop C)}_{\text{QFT}} + \frac{g^2}{4\pi} S_1(m,T) S_0(m,T)$$
$$- \frac{g}{4\pi} S_0(m,T) \left[\text{(one-loop)}_{QFT}\right] + g S_1(m,T) \frac{\partial}{\partial m^2} \text{(one-loop)}_{\text{QFT}} \tag{A12}$$

with

$$S_N(m,T) = \frac{1}{\pi} \sum_{n=1}^{\infty} \left(\frac{m}{2\pi n\beta}\right)^N K_N(nm\beta), \tag{A13}$$

$$\text{(two-loop C)}_{\text{QFT}} = -\frac{m^2 g^2}{(4\pi)^4} \left[\frac{4}{\epsilon^2} + 2\frac{\psi(1)+\psi(2)}{\epsilon} - \frac{4}{\epsilon} \ln\left(\frac{m^2}{4\pi\mu^2}\right) + \mathcal{O}(\epsilon^0)\right], \tag{A14}$$

$$\left[\text{(one-loop)}_{\text{QFT}}\right] = \frac{m^2 g}{(4\pi)^2} \left[\frac{2}{\epsilon} + \psi(2) + \ln\left(\frac{4\pi\mu^2}{m^2}\right)\right] + \mathcal{O}(\epsilon), \tag{A15}$$

$$\frac{\partial}{\partial m^2} \left[\text{(one-loop)}_{\text{QFT}}\right] = \frac{g}{(4\pi)^2} \left[\frac{2}{\epsilon} + \psi(1) + \ln\left(\frac{4\pi\mu^2}{m^2}\right)\right] + \mathcal{O}(\epsilon). \tag{A16}$$

4. Diagram two loop D

The integral expression for sunset/sunrise diagram can be written in ITF as

$$I = \text{(sunset)}_{\text{ITF}} = \lambda^2 T^2 \int \sum_{n_p=-\infty}^{\infty} \sum_{n_q=-\infty}^{\infty} \frac{1}{\omega_{n_p}^2 + \varepsilon_p^2} \frac{(2\pi)^3}{\omega_{n_q}^2 + \varepsilon_q^2} \frac{\delta^3(p+q+r+s)}{\omega_{n_p+n_q+n_s}^2 + \varepsilon_r^2} \frac{d^3p}{(2\pi)^3} \frac{d^3q}{(2\pi)^3} \frac{d^3r}{(2\pi)^3}. \tag{A17}$$

From [44,46] the integral can be expressed as $I = I_1 + I_2 + I_3$ where

$$I_1 = \text{(sunset)}_{QFT} = \int \frac{\lambda^2}{P^2+m^2} \frac{1}{Q^2+m^2} \frac{1}{R^2+m^2} (2\pi)^4 \delta^4(P+Q+R+S) \frac{d^4P}{(2\pi)^4} \frac{d^4Q}{(2\pi)^4} \frac{d^4R}{(2\pi)^4} \tag{A18}$$

with $S = [\omega_{n_s}, \vec{s}]$,

$$I_2 = \int \frac{d^3p}{(2\pi)^3} \frac{3n_B(\beta\varepsilon_p)}{2\varepsilon_p} \sum_{\sigma_1=\pm 1} \bigcirc\!\!\times\!\!\bigcirc \left((P+S)^2\right)_{QFT}$$

with

$$P = [i\sigma_1\varepsilon_p, \vec{p}], \qquad S = [\omega_{n_s}, \vec{s}],$$

and

$$\bigcirc\!\!\times\!\!\bigcirc_{\mathrm{QFT}}(K^2) = \int \frac{\lambda^2}{R^2+m^2}\frac{1}{Q^2+m^2}(2\pi)^4\delta^4(R+Q+K)\frac{d^4R}{(2\pi)^4}\frac{d^4Q}{(2\pi)^4}. \tag{A19}$$

Similarly

$$I_3 = \lambda^2 \int \frac{d^3p}{(2\pi)^3}\frac{d^3q}{(2\pi)^3}\frac{3n_B(\beta\varepsilon_p)n_B(\beta\varepsilon_q)}{4\varepsilon_p\varepsilon_q} \times \sum_{\sigma_1,\sigma_2=\pm 1} \frac{1}{(i\sigma_1\varepsilon_p + i\sigma_2\varepsilon_q + \omega_{n_s})^2 + (\vec{p}+\vec{q}+\vec{s})^2 + m^2}$$

with

$$P = [i\sigma_1\varepsilon_p, \vec{p}], \qquad Q = [i\sigma_2\varepsilon_q, \vec{q}], \qquad S = [\omega_{n_s}, \vec{s}]. \tag{A20}$$

Now by taking the corresponding result from [34] and Appendix A-2, we can write

$$\bigcirc_{\mathrm{ITF}} = \bigcirc_{\mathrm{QFT},S_0=\omega_{n_s}} + \int \frac{d^3p}{(2\pi)^3}\frac{3n_B(\beta\varepsilon_p)}{2\varepsilon_p} \sum_{\sigma_1} \bigcirc\!\!\times\!\!\bigcirc_{\mathrm{QFT}}(P+S)^2 + I_3, \tag{A21}$$

where

$$\bigcirc_{\mathrm{QFT},s_0=\omega_{n_s}} = -g^2\frac{m^2}{(4\pi)^4}\left(\frac{6}{\epsilon^2} + \frac{S^2}{2m^2\epsilon}\right) - g^2\frac{m^2}{(4\pi)^4}\frac{6}{\epsilon}\left[\frac{3}{2} + \psi(1) + \ln\left(\frac{4\pi\mu^2}{m^2}\right)\right] + \mathcal{O}(\epsilon) \tag{A22}$$

with $S^2 = \omega_{n_s}^2 + s^2$,

$$\begin{aligned}\{g^2\mu^\epsilon\}\sum_{\sigma_1} \bigcirc\!\!\times\!\!\bigcirc_{\mathrm{QFT}}(P+S) = {} & \frac{2g^2\mu^\epsilon}{(4\pi)^2}\left(\frac{2}{\epsilon} + \psi(1)\right) \\ & + \sum_{\sigma=\pm 1}\frac{g^2\mu^\epsilon}{(4\pi)^2}\left(\int_0^1 dx \ln\left[\frac{4\pi\mu^2}{[(i\sigma\varepsilon_p + \omega_{n_s})^2 + (p+s)^2]x(1-x) + m^2}\right]\right) + \mathcal{O}(\epsilon).\end{aligned} \tag{A23}$$

When $S = 0$,

$$\{g^2\mu^\epsilon\}\sum_{\sigma_1} \bigcirc\!\!\times\!\!\bigcirc_{\mathrm{QFT}} = \frac{2g^2\mu^\epsilon}{(4\pi)^2}\left(\frac{2}{\epsilon} + \psi(1)\right) - \frac{2g^2\mu^\epsilon}{(4\pi)^2}\left(\int_0^1 dx \ln\left[1 - x + x^2\right]\right) + \frac{2g^2\mu^\epsilon}{(4\pi)^2}\ln\left(\frac{4\pi\mu^2}{m^2}\right) + \mathcal{O}(\epsilon). \tag{A24}$$

Now combining results, we can write it as in the case of the pole term, i.e.,

$$\begin{aligned}\mathcal{K}\left(\bigcirc_{\mathrm{ITF}}\right) &= \mathcal{K}\left(\bigcirc_{\mathrm{QFT},k_0=\omega_{n_k}}\right) + 3S_1(m,T)\ \mathcal{K}\left(\bigcirc\!\!\times\!\!\bigcirc_{\mathrm{QFT}}\right) \\ &= \mathcal{K}\left(\bigcirc_{\mathrm{QFT},k_0=\omega_{n_k}}\right) + 3gS_1(m,T)\ \frac{\partial}{\partial m^2}\mathcal{K}\left(\bigcirc\!\!-\!\!\bigcirc_{\mathrm{QFT}}\right).\end{aligned} \tag{A25}$$

When external momentum $S = 0$, the integral result is

$$\text{ITF},S=0 = \text{QFT},S=0 + 3S_1(m,T)\ \mathcal{K}\left(\text{QFT}\right) + 3S_1(m,T)\frac{g^2\mu^\epsilon}{(4\pi)^2}\left(\psi(1)+2-\frac{\sqrt{3}\pi}{3}+\ln\left(\frac{4\pi\mu^2}{m^2}\right)\right) + \frac{3g^2m^2}{32\pi^4}\int_0^\infty\int_0^\infty U(x)U(y)G(x,y)\,dx\,dy \tag{A26}$$

with

$$U(x)=\frac{\sinh(x)}{\exp(\beta m\cosh(x))-1},\quad G(x,y)=\ln\left(\frac{1+2\cosh(x-y)}{1+2\cosh(x+y)}\frac{1-2\cosh(x+y)}{1-2\cosh(x-y)}\right),\quad \int_0^1\ln(1-x+x^2)dx=\frac{\sqrt{3}\pi}{3}-2. \tag{A27}$$

The approximation can be verified using results from [46].

5. Diagram two loop E

$$\text{ITF} = -\frac{1}{\lambda}\left[\lambda^2 T\sum_{n_p=-\infty}^{\infty}\int\frac{d^3p}{(2\pi)^3}\frac{1}{\varepsilon_{p-r}^2+\omega_{n_p-n_r}^2}\ \frac{1}{\varepsilon_p^2+\omega_{n_p}^2}\right]^2 = -\frac{1}{\lambda}\left[\text{ITF}\right]^2.$$

Using results from Appendix A-2

$$= -\frac{1}{\lambda}\left[\text{QFT} + \lambda^2\sum_{\sigma,\sigma_1=\pm1}\int\frac{n_B(\beta\varepsilon_p)}{2\varepsilon_p\varepsilon_{p+r}}\frac{1}{\sigma_1\varepsilon_p+\varepsilon_{p+r}+i\sigma\omega_{n_r}}\frac{d^3p}{(2\pi)^3}\right]^2.$$

If we put

$$W(r,n_r)=\sum_{\sigma,\sigma_1=\pm1}\int\frac{n_B(\beta\varepsilon_p)}{2\varepsilon_p\varepsilon_{p+r}}\frac{1}{\sigma_1\varepsilon_p+\varepsilon_{p+r}+i\sigma\omega_{n_r}}\frac{d^3p}{(2\pi)^3}, \tag{A28}$$

then

$$\text{ITF} = \text{QFT},r_0=\omega_{n_r} - 2gW(r,n_r)\left[\text{QFT},r_0=\omega_{n_r}\right] - (g\mu^\epsilon)^3\,W^2(r,n_r). \tag{A29}$$

If we take results from [34] and previous sections, we can write

$$\text{QFT},k_0=\omega_{n_k} = -\lambda^3\int\frac{d^Np}{(2\pi)^N}\frac{1}{(p-k)^2+m^2}\frac{1}{p^2+m^2}\int\frac{d^Nq}{(2\pi)^N}\frac{1}{(q-k)^2+m^2}\frac{1}{q^2+m^2}.$$

Setting $\lambda = g\mu^\epsilon$, and as $N\to 4-\epsilon$, (A30)

$$= -g\mu^\epsilon\frac{g^2}{(4\pi)^4}\left(\frac{4}{\epsilon^2}+\frac{4}{\epsilon}\psi(1)\right) - g\mu^\epsilon\frac{g^2}{(4\pi)^4}\frac{4}{\epsilon}\int_0^1 dx\ln\left[\frac{4\pi\mu^2}{K^2x(1-x)+m^2}\right]+\mathcal{O}(\epsilon^0)$$

and $K^2=\omega_{n_k}^2+k^2$ from Appendix A-2

$$\text{QFT} = \frac{g^2\mu^\epsilon}{(4\pi)^2}\left(\frac{2}{\epsilon}+\psi(1)+\int_0^1 dx\ln\left[\frac{4\pi\mu^2}{K^2x(1-x)+m^2}\right]+\mathcal{O}(\epsilon)\right). \tag{A31}$$

6. Diagram two loop F

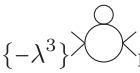

$$
\begin{aligned}
\{-\lambda^3\}\,\text{ITF} &= -\lambda^3 T^2 \sum_{n_p=-\infty}^{\infty} \int \frac{d^3p}{(2\pi)^3} \frac{1}{\varepsilon_{p-r}^2 + \omega_{n_p-n_r}^2} \frac{1}{(\varepsilon_p^2 + \omega_{n_p}^2)^2} \sum_{n_q=-\infty}^{\infty} \int \frac{d^3q}{(2\pi)^3} \frac{1}{\varepsilon_q^2 + \omega_{n_q}^2} \\
&= \left[-\frac{1}{2} \frac{\partial}{\partial m^2} \sum_{n_p=-\infty}^{\infty} \int \frac{d^3p}{(2\pi)^3} \frac{1}{\varepsilon_{p-r}^2 + \omega_{n_p-n_r}^2} \frac{\lambda^2 T}{\varepsilon_p^2 + \omega_{n_p}^2} \right] \times \sum_{n_q=-\infty}^{\infty} \int \frac{d^3q}{(2\pi)^3} \frac{-\lambda T}{\varepsilon_q^2 + \omega_{n_q}^2} \\
&= \{-\lambda\}\,\text{ITF} \times -\frac{1}{2} \frac{\partial}{\partial m^2} \left[\{\lambda^2\}\,\text{ITF} \right] \\
&= \left(\{-\lambda\}\,\text{QFT} - \lambda S_1(m,T) \right) \times -\frac{1}{2} \frac{\partial}{\partial m^2} \left[\{\lambda^2\}\,\text{QFT} + \lambda^2 W(r,n_r) \right] \\
&= \{-\lambda\}\,\text{QFT} \times -\frac{1}{2} \frac{\partial}{\partial m^2} \left[\{\lambda^2\}\,\text{QFT} \right] + (\cdots).
\end{aligned}
\tag{A32}
$$

Solving we get

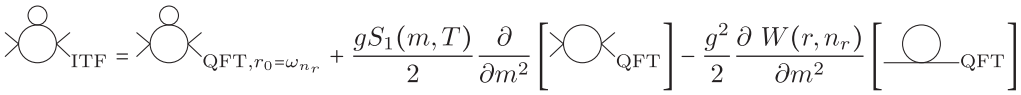

$$
\begin{aligned}
\text{ITF} &= \text{QFT}, r_0=\omega_{n_r} + \frac{g S_1(m,T)}{2} \frac{\partial}{\partial m^2} \left[\text{QFT} \right] - \frac{g^2}{2} \frac{\partial\, W(r,n_r)}{\partial m^2} \left[\text{QFT} \right] \\
&\quad + g^3 \frac{S_1(m,T)}{2} \frac{\partial}{\partial m^2} W(r,n_r).
\end{aligned}
\tag{A33}
$$

Using [34] and results from Appendixes A-1 and A-2 we can write

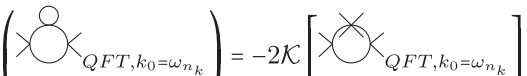

$$
\mathcal{K}\left(QFT, k_0=\omega_{n_k} \right) = -2\mathcal{K}\left[QFT, k_0=\omega_{n_k} \right]
\tag{A34}
$$

and $K^2 = \omega_{n_k}^2 + k^2$,

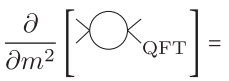

$$
\frac{\partial}{\partial m^2} \left[\text{QFT} \right] = -\frac{g^2 \mu^\epsilon}{(4\pi)^2} \int_0^1 \frac{1}{K^2 x(1-x) + m^2} dx,
\tag{A35}
$$

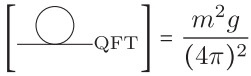

$$
\left[\text{QFT} \right] = \frac{m^2 g}{(4\pi)^2} \left[\frac{2}{\epsilon} + \psi(2) + \ln\left(\frac{4\pi\mu^2}{m^2} \right) \right] + \mathcal{O}(\epsilon).
\tag{A36}
$$

7. Diagram two loop G

We have to evaluate

$$
= \int \sum_{n=-\infty}^{\infty} \sum_{\theta=-\infty}^{\infty} \frac{-\lambda^3}{\omega_n^2 + \varepsilon_p^2} \frac{T^2}{\omega_\theta^2 + \varepsilon_q^2} \frac{1}{\omega_{n-\alpha}^2 + \varepsilon_r^2} \frac{(2\pi)^6 \delta^6}{\omega_{n-\theta+\eta}^2 + \varepsilon_s^2} \frac{d^3r}{(2\pi)^3} \frac{d^3s}{(2\pi)^3} \frac{d^3p}{(2\pi)^3} \frac{d^3q}{(2\pi)^3},
\tag{A37}
$$

where $\delta^6 = \delta^3(\vec{r} + \vec{p} - \vec{k_1} - \vec{k_2}) \delta^3(\vec{s} + \vec{q} - \vec{p} - \vec{k_3})$.

The result expanded as the summation

$$
= I_{11} + I_{21} + I_{22} + 2I_{F1} + 2I_{F2} + 2I_{F3} + I_{F4},
\tag{A38}
$$

where

$$I_{11} = \int \frac{1}{P^2+m^2}\frac{1}{Q^2+m^2}\frac{1}{R^2+m^2}\frac{1}{S^2+m^2}\frac{d^4P}{(2\pi)^4}\frac{d^4Q}{(2\pi)^4}\frac{d^4R}{(2\pi)^4}\frac{d^4S}{(2\pi)^4} \times (2\pi)^4\delta^4(R+P-K_1-K_2)(2\pi)^4\delta^4(S+Q-P-K_3) \tag{A39}$$

with

$$R=[r_0,\vec{r}], \qquad P=[p_0,\vec{p}], \qquad K_1+K_2=[\omega_\alpha,\vec{k}_1+\vec{k}_2], \qquad K_3=[\omega_\eta,\vec{k}_3]. \tag{A40}$$

We define

$$J(K^2) = \int \frac{1}{P^2+m^2}\frac{1}{(P-K)^2+m^2}\frac{d^4P}{(2\pi)^4}, \tag{A41}$$

$$L(A,B,C) = \frac{1}{A^2+m^2}\frac{1}{B^2+m^2}\frac{1}{C^2+m^2}, \tag{A42}$$

and

$$G(A,B) = \frac{1}{A^2+m^2}\frac{1}{B^2+m^2}. \tag{A43}$$

Then

$$I_{21} = \int \frac{d^3p}{(2\pi)^3}\frac{n_B(\beta\varepsilon_p)}{2\varepsilon_p}\sum_{\sigma=\pm1}\left[\frac{J[(P+K_3)^2]}{(P-K_1-K_2)^2+m^2}\right]_{p_0=-i\sigma\varepsilon_p}. \tag{A44}$$

Similarly

$$I_{22} = \int \frac{d^3r}{(2\pi)^3}\frac{n_B(\beta\varepsilon_r)}{2\varepsilon_r}\sum_{\sigma=\pm1}\left[\frac{J[(K_1+K_2+K_3-R)^2]}{(R-K_1-K_2)^2+m^2}\right]_{r_0=-i\sigma\varepsilon_r}, \tag{A45}$$

$$I_{F1} = \int \frac{d^3q}{(2\pi)^3}\frac{n_B(\beta\varepsilon_q)}{2\varepsilon_q}\sum_{\sigma=\pm1}L(R-K_1-K_2,R,R+Q-K_1-K_2-K_3)\frac{d^4R}{(2\pi)^4}_{q_0=i\sigma\varepsilon_q}, \tag{A46}$$

$$I_{F2} = \int \frac{d^3p}{(2\pi)^3}\frac{n_B(\beta\varepsilon_p)}{2\varepsilon_p}\frac{d^3q}{(2\pi)^3}\frac{n_B(\beta\varepsilon_q)}{2\varepsilon_q}\sum_{\sigma_1,\sigma_3=\pm1}G(P-K_1-K_2,Q-P-K_3)|^{q_0=i\sigma_3\varepsilon_q}_{p_0=i\sigma_1\varepsilon_p}, \tag{A47}$$

$$I_{F3} = \int \frac{d^3s}{(2\pi)^3}\frac{d^3r}{(2\pi)^3}\frac{n_B(\beta\varepsilon_s)n_B(\beta\varepsilon_r)}{4\varepsilon_s\varepsilon_r}\sum_{\sigma_1,\sigma_3=\pm1}G(R-K_1-K_2,S+R-K_1-K_2-K_3)|^{r_0=i\sigma_3\varepsilon_r}_{s_0=i\sigma_1\varepsilon_s}, \tag{A48}$$

$$I_{F4} = \int \frac{d^3q}{(2\pi)^3}\frac{d^3s}{(2\pi)^3}\frac{n_B(\beta\varepsilon_s)n_B(\beta\varepsilon_q)}{4\varepsilon_s\varepsilon_q}\sum_{\sigma_1,\sigma_3=\pm1}G(S+Q-K_3,Q+S+K_1+K_2-K_3)|^{s_0=i\sigma_3\varepsilon_s}_{q_0=i\sigma_1\varepsilon_q}. \tag{A49}$$

If we look at the integral, we can find one thing: the first three terms, I_{11}, I_{21}, and I_{22}, diverge, the rest become finite. i.e., $\mathrm{I} = I_{11}+I_{21}+I_{22}+$ Finite terms $(2I_{F1}+2I_{F2}+2I_{F3}+I_{F4})$. If we define the pole finding operator $\mathcal{K}$, then by the structure, we can write

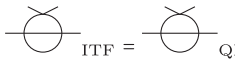

(A50)

$$\mathcal{K}\left[\{-\lambda^3\}\;\text{  }_{\mathrm{ITF}}\right]=\mathcal{K}\left[\{-\lambda^3\}\;\text{ 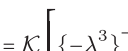 }_{\mathrm{QFT},k_0=\omega_{n_k}}\right]$$
$$-\left(\lambda\int\frac{d^3p}{(2\pi)^3}\frac{n_B(\beta\varepsilon_p)}{2\varepsilon_p}\times\mathcal{K}\left[\{\lambda^2\}\sum_{\sigma=\pm1}\text{ 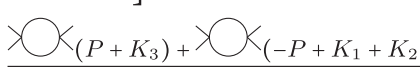 }_{p_0=-i\sigma\varepsilon_p}\right]\right). \tag{A51}$$

We rewrite

$$\begin{aligned}\int_{-1}^{1}d\cos\theta\sum_{\sigma=\pm1}\frac{1}{(P-K)^2+m^2}&=\int_{-1}^{1}d\cos\theta\sum_{\sigma=\pm1}\frac{1}{(p-k)^2+(i\sigma\varepsilon_p+\omega_\alpha)^2+m^2}\\&=\int_{-1}^{1}d\cos\theta\frac{2(k^2-2pk\cos\theta+\omega_\alpha^2)}{(k^2-2pk\cos\theta+\omega_\alpha^2)^2+4\varepsilon_p^2\omega_\alpha^2}\\&=\int_{-1}^{1}d\cos\theta\frac{2(k^2+2pk\cos\theta+\omega_\alpha^2)}{(k^2+2pk\cos\theta+\omega_\alpha^2)^2+4\varepsilon_p^2\omega_\alpha^2},\end{aligned} \tag{A52}$$

$$W(r,n_r)=\int\frac{d^3p}{(2\pi)^3}\frac{2n_B(\beta\varepsilon_p)}{\varepsilon_p}\frac{r^2+2pr\cos\theta+\omega_{n_r}^2}{(r^2+2pr\cos\theta+\omega_{n_r}^2)^2+4\varepsilon_p^2\omega_{n_r}^2}. \tag{A53}$$

We know that from Appendix A-2

$$\mathcal{K}\left(\text{  }_{\mathrm{QFT}}\right)=\frac{g^2\mu^\epsilon}{(4\pi)^2}\left(\frac{2}{\epsilon}\right). \tag{A54}$$

So

$$\mathcal{K}\left[\text{  }_{\mathrm{ITF}}\right]=\mathcal{K}\left[\text{  }_{\mathrm{QFT},k_{0i}=\omega_{n_i}}\right]$$
$$-g\mu^\epsilon\left(\int\frac{d^3p}{(2\pi)^3}\frac{2n_B(\beta\varepsilon_p)}{\varepsilon_p}\frac{(k^2+2pk\cos\theta+\omega_\alpha^2)}{(k^2+2pk\cos\theta+\omega_\alpha^2)^2+4\varepsilon_p^2\omega_\alpha^2}\mathcal{K}\left(\text{}_{\mathrm{QFT}}\right)\right). \tag{A55}$$

So the pole term relation can be written as

$$\mathcal{K}\left[\text{  }_{\mathrm{ITF}}\right]=\mathcal{K}\left[\text{  }_{\mathrm{QFT},k_{0i}=\omega_{n_i}}\right]-g\mu^\epsilon W(k_i,n_{k_i})\mathcal{K}\left(\text{}_{\mathrm{QFT}}\right), \tag{A56}$$

where

$$\mathcal{K}\left[\text{ 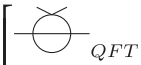 }_{QFT}\right]=g\mu^\epsilon\frac{g^2}{(4\pi)^4}\frac{2}{\epsilon^2}\left(1+\frac{\epsilon}{2}+\epsilon\;\psi(1)\right)-g\mu^\epsilon\frac{g^2}{(4\pi)^4}\frac{2}{\epsilon}\int_0^1dx\ln\left[\frac{(K_1+K_2)^2x(1-x)+m^2}{4\pi\mu^2}\right] \tag{A57}$$

with $K_i=[\omega_{n_{k_i}},\vec{k}_i]$.

APPENDIX B: COUNTERTERM DIAGRAMS

1. Counterterm 1

From [34], the counterterm for divergence for the four-point function derived is

$$\text{ 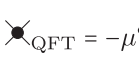 }_{\mathrm{QFT}}=-\mu^\epsilon g c_g^1=-\frac{3}{2}\mathcal{K}\left(\text{}_{\mathrm{QFT}}\right). \tag{B1}$$

The corresponding diagram in imaginary time formalism is

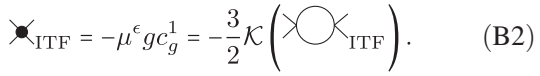

(B2)

From Appendix A-2, one can find that the diverging term is the same for the diagram in imaginary time formalism and nonthermal QFT; thus, we can write

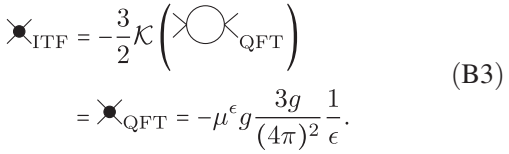

(B3)

2. Counterterm 2

From [34] defining the $*$ operator, the substitution of the counterterm $-m^2 c_{m^2}$ or $-\mu^\epsilon g c_g$, we can express counterterms as

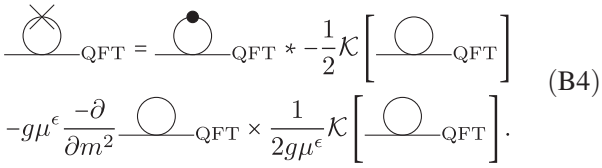

(B4)

We have from Appendix A-1 the relation

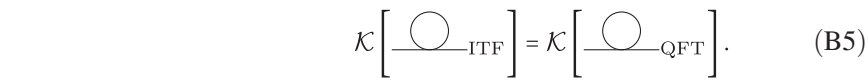

(B5)

So, for ITF, the corresponding derivation is

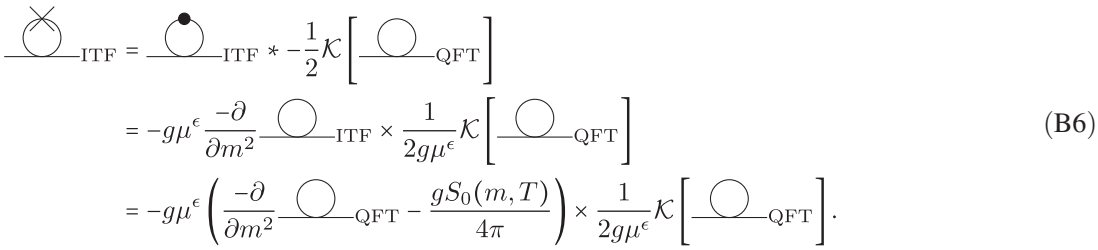

(B6)

So

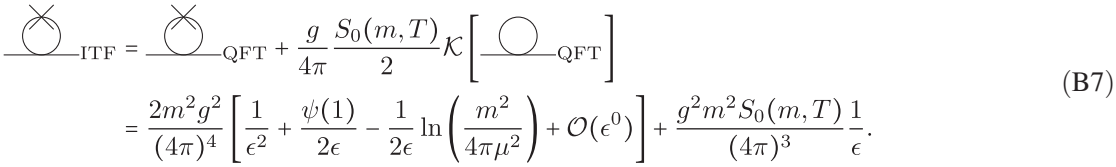

(B7)

3. Counterterm 3

From [34], the calculation proceeds as

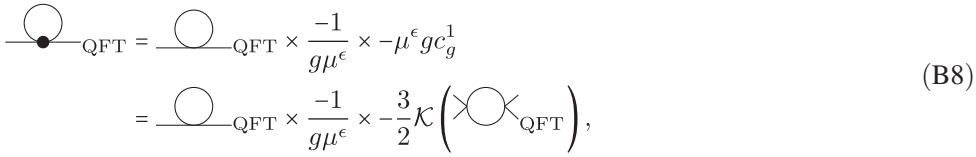

(B8)

and the corresponding diagram made with results from Appendixes A-1 and A-2 is

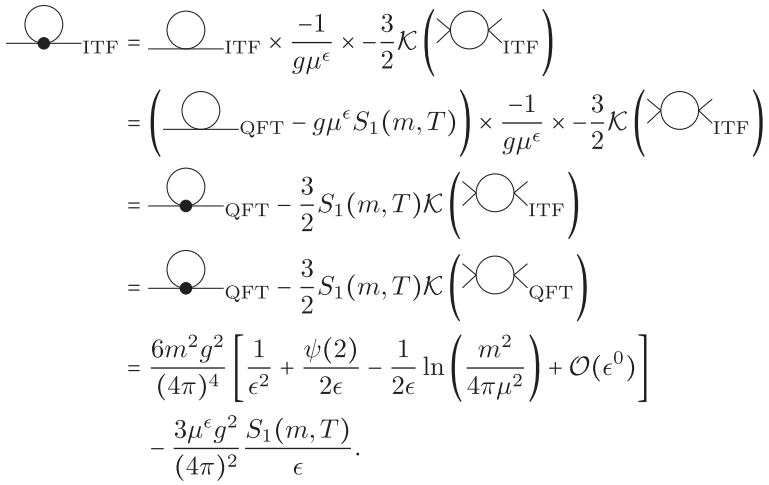

$$
\begin{aligned}
&= \left(\quad_{\mathrm{QFT}} - g\mu^{\epsilon} S_1(m,T) \right) \times \frac{-1}{g\mu^{\epsilon}} \times -\frac{3}{2}\mathcal{K}\left(\quad_{\mathrm{ITF}} \right) \\
&= \quad_{\mathrm{QFT}} - \frac{3}{2} S_1(m,T)\mathcal{K}\left(\quad_{\mathrm{ITF}} \right) \\
&= \quad_{\mathrm{QFT}} - \frac{3}{2} S_1(m,T)\mathcal{K}\left(\quad_{\mathrm{QFT}} \right) \\
&= \frac{6m^2 g^2}{(4\pi)^4}\left[\frac{1}{\epsilon^2} + \frac{\psi(2)}{2\epsilon} - \frac{1}{2\epsilon}\ln\left(\frac{m^2}{4\pi\mu^2} \right) + \mathcal{O}(\epsilon^0) \right] \\
&\quad - \frac{3\mu^{\epsilon} g^2}{(4\pi)^2}\frac{S_1(m,T)}{\epsilon}.
\end{aligned}
\tag{B9}
$$

4. Counterterm 4

From [34], the diagram evaluated is

$$
\mathcal{K}\left[\quad \right]_{\mathrm{QFT}} = \mathcal{K}\left[\quad_{\mathrm{QFT}} * -\frac{3}{2}\mathcal{K}\left(\quad \right)_{\mathrm{QFT}} \right]. \tag{B10}
$$

Using the results of Appendix A-2 the corresponding diagram in ITF can be written as

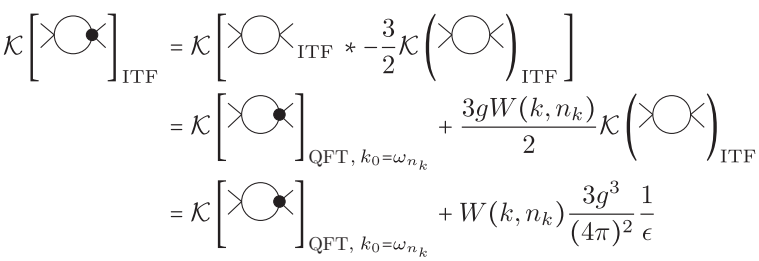

$$
\begin{aligned}
\mathcal{K}\left[\quad \right]_{\mathrm{ITF}} &= \mathcal{K}\left[\quad_{\mathrm{ITF}} * -\frac{3}{2}\mathcal{K}\left(\quad \right)_{\mathrm{ITF}} \right] \\
&= \mathcal{K}\left[\quad \right]_{\mathrm{QFT},\, k_0=\omega_{n_k}} + \frac{3gW(k,n_k)}{2}\mathcal{K}\left(\quad \right)_{\mathrm{ITF}} \\
&= \mathcal{K}\left[\quad \right]_{\mathrm{QFT},\, k_0=\omega_{n_k}} + W(k,n_k)\frac{3g^3}{(4\pi)^2}\frac{1}{\epsilon}
\end{aligned}
\tag{B11}
$$

with

$$
\mathcal{K}\left[\quad \right]_{\mathrm{QFT},k_0=\omega_{n_k}} = \frac{\mu^{\epsilon} g^3}{(4\pi)^4}\left[\frac{6}{\epsilon^2} + \frac{3\psi(1)}{\epsilon} - \frac{3}{\epsilon}\int_0^1 \ln\left[\frac{m^2 + K^2(x(1-x))}{4\pi\mu^2} \right] dx \right], \tag{B12}
$$

where $K^2 = k^2 + \omega_{n_k}^2$.

5. Counterterm 5

From [34], one can derive the diagram as

$$\mathcal{K}\left[\text{ 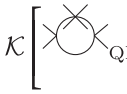 }_{\mathrm{QFT}}\right] = \mathcal{K}\left(-\lambda^3 \int \frac{1}{(P^2+m^2)^2}\frac{1}{(P-K)^2+m^2}\frac{d^4P}{(2\pi)^4} \times -m^2 c^1_{m^2} \times \frac{-1}{g\mu^\epsilon}\right)$$
$$= \mathcal{K}\left(\frac{\lambda}{2}\frac{\partial}{\partial m^2}\lambda^2 \int \frac{1}{(P^2+m^2)}\frac{1}{(P-K)^2+m^2}\frac{d^4P}{(2\pi)^4} \times -m^2 c^1_{m^2} \times \frac{-1}{g\mu^\epsilon}\right)$$
$$= \mathcal{K}\left(-g\mu^\epsilon \times -\frac{1}{2}\frac{\partial}{\partial m^2}\text{ 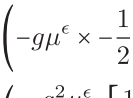 }_{\mathrm{QFT}} \times \frac{-1}{\mu^\epsilon g} \times -\frac{1}{2}\mathcal{K}\left[\text{}_{\mathrm{QFT}}\right]\right) \tag{B13}$$
$$= \mathcal{K}\left(-\frac{g^2\mu^\epsilon}{(4\pi)^2}\left[\frac{1}{2}\int_0^1 \frac{1}{K^2x(1-x)+m^2}\,dx\right] \times \frac{m^2 g}{(4\pi)^2}\frac{1}{\epsilon}\right)$$
$$= -\frac{1}{2}\mathcal{K}\left(\text{  }_{\mathrm{QFT},k_0=\omega_{n_k}}\right).$$

The corresponding counterterm in imaginary time formalism can be written with Appendixes A-2 and A-1 as

$$\mathcal{K}\left[\text{  }_{\mathrm{ITF}}\right] = \mathcal{K}\left(-g\mu^\epsilon \times -\frac{1}{2}\frac{\partial}{\partial m^2}\text{ 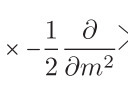 }_{\mathrm{ITF}} \times \frac{-1}{\mu^\epsilon g} \times -\frac{1}{2}\mathcal{K}\left[\text{}_{\mathrm{ITF}}\right]\right)$$
$$= \mathcal{K}\left(-g\mu^\epsilon\left(-\frac{1}{2}\frac{\partial}{\partial m^2}\text{ 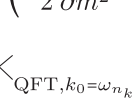 }_{\mathrm{QFT}} - \frac{g^2}{2}\frac{\partial W(k,n_k)}{\partial m^2}\right)\frac{-1}{\mu^\epsilon g} \times \frac{-1}{2}\mathcal{K}\left[\text{}_{\mathrm{QFT}}\right]\right) \tag{B14}$$
$$= \mathcal{K}\left(\text{ 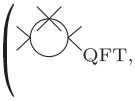 }_{\mathrm{QFT},k_0=\omega_{n_k}}\right) + \frac{1}{4}g^2\left(\frac{\partial W(k,n_k)}{\partial m^2}\right)\mathcal{K}\left[\text{}_{\mathrm{QFT}}\right] = -\frac{1}{2}\mathcal{K}\left(\text{ 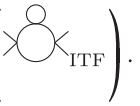 }_{\mathrm{ITF}}\right).$$

It can also be derived using the * operation [34], i.e.,

$$\mathcal{K}\left[\text{ 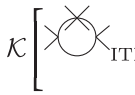 }_{\mathrm{ITF}}\right] = \mathcal{K}\left(\text{ 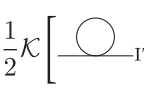 }_{\mathrm{ITF}} * -\frac{1}{2}\mathcal{K}\left[\text{}_{\mathrm{ITF}}\right]\right). \tag{B15}$$

APPENDIX C: RENORMALIZATION CONSTANTS

We have from [34]

$$\gamma(g) = -Z_{\phi,1} = -\epsilon c_\phi, \tag{C1}$$

$$\gamma_m(g) = \frac{1}{2}\frac{g}{(4\pi)^2} - \frac{1}{2}\frac{g^2}{(4\pi)^4} + \gamma(g), \tag{C2}$$

$$\beta(g) = -\epsilon g + \frac{3g^2}{(4\pi)^2} - \frac{6g^3}{(4\pi)^4} + 4g\gamma(g). \tag{C3}$$

1. Case 1: $K \neq 0$

In this case as per Eq. (64)

$$K^2 c_\phi = -\frac{g^2}{(4\pi)^4}\frac{K^2}{12}\frac{1}{\epsilon}. \tag{C4}$$

Equations (C1) to (C3) become

$$\gamma(g) = \frac{g^2}{(4\pi)^4}\frac{1}{12}, \tag{C5}$$

$$\gamma_m(g) = \frac{1}{2}\frac{g}{(4\pi)^2} - \frac{5}{12}\frac{g^2}{(4\pi)^4}, \tag{C6}$$

$$\beta(g) = -\epsilon g + \frac{3g^2}{(4\pi)^2} - \frac{17g^3}{3(4\pi)^4}. \tag{C7}$$

2. Case 2: $K = 0$

Now Eqs. (C1) to (C3) change because of

$$K^2 c_\phi = 0. \tag{C8}$$

So

$$\gamma(g) = 0, \tag{C9}$$

$$\gamma_m(g) = \frac{1}{2}\frac{g}{(4\pi)^2} - \frac{1}{2}\frac{g^2}{(4\pi)^4}, \tag{C10}$$

$$\beta(g) = -\epsilon g + \frac{3g^2}{(4\pi)^2} - \frac{6g^3}{(4\pi)^4}. \tag{C11}$$

3. Relation

We can relate them as

$$\gamma(g)_{k=0} = \gamma(g)_{k\neq 0} - \frac{g^2}{(4\pi)^4}\frac{1}{12} = 0, \tag{C12}$$

$$\gamma_m(g)_{k=0} = \gamma_m(g)_{k\neq 0} - \frac{g^2}{(4\pi)^4}\frac{1}{12}, \tag{C13}$$

$$\beta(g)_{k=0} = \beta(g)_{k\neq 0} - \frac{1}{3}\frac{g^3}{(4\pi)^4}. \tag{C14}$$

APPENDIX D: COUPLING CONSTANT FORM DERIVATION

We have

$$\begin{aligned}\Gamma^{\text{diff}}_{n_k,\vec{k}=0} = {} & \frac{g}{2}S_1(m,T) - \frac{3g^2}{4}\frac{S_1(m,T)}{(4\pi)^2}\left[\psi(1) + \ln\left(\frac{4\pi\mu^2}{m^2}\right)\right] \\ & - \frac{g^2}{4(4\pi)}S_0(m,T)S_1(m,T) \\ & + \frac{g^2m^2}{4(4\pi)^3}S_0(m,T)\left[\psi(2) + \ln\left(\frac{4\pi\mu^2}{m^2}\right)\right] \\ & - \frac{g^2m^2}{64\pi^4}Y(m,T) - \frac{g^2}{32\pi^2}S_1(m,T)\left[2 - \frac{\pi}{\sqrt{3}}\right].\end{aligned} \tag{D1}$$

Let us express

$$\Gamma^{\text{diff}}_{n_k,\vec{k}=0} = gT_1 + g^2T_2, \tag{D2}$$

$$\frac{\partial}{\partial \ln\mu}\Gamma^{\text{diff}}_{n_k,\vec{k}=0} = gT_{1,\ln\mu} + g^2T_{2,\ln\mu}, \tag{D3}$$

$$\frac{\partial}{\partial \ln m}\Gamma^{\text{diff}}_{n_k,\vec{k}=0} = gT_{1,\ln m} + g^2T_{2,\ln m} \tag{D4}$$

with

$$S_N(m,T) = \frac{1}{\pi}\sum_{n=1}^{\infty}\left(\frac{m}{2\pi n\beta}\right)^N K_N(nm\beta), \tag{D5}$$

$$\begin{aligned}T_1 &= \frac{1}{2}S_1(m,T), \\ T_2 &= V_1(m,T) + V_2(m,T)\ln(\mu),\end{aligned} \tag{D6}$$

$$T_{1,\ln\mu} = 0, \tag{D7}$$

$$T_{1,\ln m} = -\frac{m^2}{4\pi}S_0(m,T), \tag{D8}$$

$$T_{2,\ln\mu} = V_2(m,T), \tag{D9}$$

$$T_{2,\ln m} = V_{1,\ln m} + V_{2,\ln m}\ln\mu, \tag{D10}$$

$$\begin{aligned}V_1(m,T) = {} & \frac{m^2}{4(4\pi)^3}S_0(m,T)\left[\psi(2) + \ln\left(\frac{4\pi}{m^2}\right)\right] - \frac{3}{4}\frac{S_1(m,T)}{(4\pi)^2}\left[\psi(1) + \ln\left(\frac{4\pi}{m^2}\right)\right] \\ & - \frac{1}{4(4\pi)}S_0(m,T)S_1(m,T) - \frac{m^2}{64\pi^4}Y(m,T) - \frac{S_1(m,T)}{32\pi^2}\left[2 - \frac{\sqrt{3}\pi}{3}\right],\end{aligned} \tag{D11}$$

$$V_2(m,T) = \left(\frac{m^2}{2(4\pi)^3}S_0(m,T) - \frac{3S_1(m,T)}{2(4\pi)^2}\right), \tag{D12}$$

$$V_{2,\ln m} = \frac{4m^2S_0(m,T)}{(4\pi)^3} - \frac{m^4S_{-1}(m,T)}{(4\pi)^4}, \tag{D13}$$

$$V_{1,\ln m} = \frac{2m^2}{(4\pi)^3} S_0(m,T)\left[\psi(1) + \ln\left(\frac{4\pi}{m^2}\right)\right] - \frac{m^4}{2(4\pi)^4} S_{-1}(m,T)\left[\psi(2) + \ln\left(\frac{4\pi}{m^2}\right)\right] + \frac{3}{2}\frac{S_1(m,T)}{(4\pi)^2} + \frac{m^2 S_0^2(m,T)}{2(4\pi)^2} + \frac{m^2}{2(4\pi)^2} S_1(m,T) S_{-1}(m,T) + \frac{m^2 S_0(m,T)}{(4\pi)^3}\left[2 - \frac{\sqrt{3}\pi}{3}\right] - \frac{m^4}{32\pi^4} Y(m,T) - \frac{m^4}{32\pi^4}\frac{\partial Y(m,T)}{\partial m^2}. \tag{D14}$$

Let us define the RGE as

$$\frac{d}{d\ln\mu} = \widehat{\mathrm{RGE}} = \mu\frac{\partial}{\partial\mu} + \beta(g)\frac{\partial}{\partial g} - n\gamma(g) + \gamma_m m\frac{\partial}{\partial m} \tag{D15}$$

with

$$\beta(g) = \beta_2 g^2 + \beta_3 g^3, \tag{D16}$$

$$\gamma(g) = \gamma_2 g^2, \tag{D17}$$

$$\gamma_m(g) = \gamma_{m1} g + \gamma_{m2} g^2. \tag{D18}$$

We have to evaluate

$$\widehat{\mathrm{RGE}}\,\tilde{\Gamma}(m,g,T,\mu) \approx_{\mathrm{TLA}} 0. \tag{D19}$$

Term by term results are

$$\beta(g)\frac{\partial}{\partial g}\Gamma^{\mathrm{diff}}_{n_k,\vec{k}=0} = g^4\{2\beta_3 T_2\} + g^3\{2\beta_2 T_2 + \beta_3 T_1\} + g^2\{\beta_2 T_1\}, \tag{D20}$$

$$\gamma_m(g)\frac{\partial}{\partial\ln m}\Gamma^{\mathrm{diff}}_{n_k,\vec{k}=0} = g^4\{\gamma_{m2} T_{2,\ln m}\} + g^3\{\gamma_{m1} T_{2,\ln m} + \gamma_{m2} T_{1,\ln m}\} + g^2\{\gamma_{m1} T_{1,\ln m}\}, \tag{D21}$$

$$-2\gamma(g)\Gamma^{\mathrm{diff}}_{n_k,\vec{k}=0} = g^4\{-2\gamma_2 T_2\} + g^3\{-2\gamma_2 T_1\}, \tag{D22}$$

$$\frac{\partial}{\partial\ln\mu}\Gamma^{\mathrm{diff}}_{n_k,\vec{k}=0} = g^2 T_{2,\ln\mu} + g T_{1,\ln\mu}, \tag{D23}$$

$$\widehat{\mathrm{RGE}}\,\Gamma^{\mathrm{diff}}_{n_k,\vec{k}=0} = g^4\{2(\beta_3-\gamma_2)T_2 + \gamma_{m2} T_{2,\ln m}\} + g^3\{2\beta_2 T_2 + (\beta_3 - 2\gamma_2)T_1 + \gamma_{m1} T_{2,\ln m} + \gamma_{m2} T_{1,\ln m}\} + g^2\{\beta_2 T_1 + \gamma_{m1} T_{1,\ln m} + T_{2,\ln\mu}\} + g T_{1,\ln\mu}. \tag{D24}$$

On applying Eqs. (D6)–(D9) on the above equation, it is clear that terms that have coefficients g and g^2 are zero,

$$\widehat{\mathrm{RGE}}\,\Gamma^{\mathrm{diff}} = 0 \Rightarrow g = \frac{A(m,T)\ln\mu + B(m,T)}{C(m,T)\ln\mu + D(m,T)} \tag{D25}$$

and

$$A = [-\gamma_{m1} V_{2,\ln m} - 2\beta_2 V_2(m,T)], \tag{D26}$$

$$C = [2(\beta_3 - \gamma_2)V_2 + \gamma_{m2} V_{2,\ln m}], \tag{D27}$$

$$B = (2\gamma_2 - \beta_3)T_1 - 2\beta_2 V_1(m,T) - \gamma_{m1} V_{1,\ln m} - \gamma_{m2} T_{1,\ln m}, \tag{D28}$$

$$D = 2(\beta_3 - \gamma_2)V_1 + \gamma_{m2} V_{1,\ln m}. \tag{D29}$$

We combine with a beta coupling constant relation such as

$$\frac{dg(\mu)}{d\ln(\mu)} = \beta_2 g^2 + \beta_3 g^3 \tag{D30}$$

and give rise to the result

$$\ln(\mu) = \int^g \frac{1}{\beta_2 t^2 + \beta_3 t^3} dt = -\frac{1}{\beta_2 g} + \frac{\beta_3}{\beta_2^2}\ln\left(\beta_3 + \frac{\beta_2}{g}\right) + \ln\mu_0. \tag{D31}$$

Similarly, the corresponding running mass coupling relation is

$$\frac{d\ln(m)}{d\ln(\mu)} = \gamma_m(g). \tag{D32}$$

Combining with the above

$$\frac{\partial\ln(m)}{\partial g}\frac{dg}{d\ln(\mu)} = \gamma_m(g) \Rightarrow \frac{\partial\ln(m)}{\partial g} = \frac{\gamma_m(g)}{\beta(g)}. \tag{D33}$$

Solving by substituting

$$\frac{\partial\ln(m)}{\partial g} = \frac{\gamma_{m1} + \gamma_{m2} g}{\beta_2 g + \beta_3 g^2}, \tag{D34}$$

$$\ln\left(\frac{m}{m_0}\right) = \chi_2 + \frac{\gamma_{m1}}{\beta_2}\ln(g) + \left(\frac{\gamma_{m2}}{\beta_3} - \frac{\gamma_{m1}}{\beta_2}\right)\ln(\beta_3 g + \beta_2), \tag{D35}$$

$\ln\mu_0$, m_0, and χ_2 are the respective integration constants. Now we have three equations containing mass scale μ, coupling constant g, and running mass m, so combining Eqs. (D35), (D31), and (D25) and solving simultaneously, we get the temperature-dependent running mass and coupling constant.

1. Coupling g limit case $T \to 0$

Here we consider limit case $T \to 0$ at $m \neq 0$. In order to find the coupling nature of μ at $T \approx 0$, $\beta m \to \infty$, we have to find the rate of convergence of $A(m,T)$, $B(m,T)$, $C(m,T)$, $D(m,T)$ as $T \to 0$, because of

$$g = \frac{A(m,T)\ln\mu + B(m,T)}{C(m,T)\ln\mu + D(m,T)}. \tag{D36}$$

Here

$$\lim_{\beta m\to\infty} S_N(m,T) \to 0. \tag{D37}$$

Since both the numerator and denominator of Eq. (D36) contain $S_N(m,T)$ with varying N, the rate of convergence of the ratios is important. So

$$\lim_{\beta m\to\infty} \frac{S_{N+1}(m,T)}{S_N(m,T)} \to 0. \tag{D38}$$

As N increases, the rate of $S_N(m,T)$ convergence also increases. The convergence of $Y(m,T)$ can be found and is

$$Y(m,T) = \int_0^\infty \int_0^\infty U(x)U(y)G(x,y)dxdy, \tag{D39}$$

$$U(x) = \frac{\sinh(x)}{\exp(\beta m\cosh(x)) - 1}, \tag{D40}$$

$$G(x,y) = \ln\left(\frac{1+2\cosh(x-y)}{1+2\cosh(x+y)}\frac{2\cosh(x+y)-1}{2\cosh(x-y)-1}\right), \tag{D41}$$

$$S_N(m,T) = \frac{1}{\pi}\sum_{j=1}^{\infty}\left(\frac{m}{2\pi j\beta}\right)^N K_N(j\beta m). \tag{D42}$$

From the expression of $G(x,y)$ itself, it is clear that $G(x,y) < \ln(3)$. So,

$$Y(m,T) < \ln(3)\left[\int_0^\infty \frac{\sinh(x)}{\exp(\beta m\cosh(x)) - 1}dx\right]^2 \tag{D43}$$

$$< \ln(3)\left[\frac{2\pi}{m}S_{\frac{1}{2}}(m,T)\right]^2. \tag{D44}$$

Therefore

$$\lim_{\beta m\to\infty} \frac{Y(m,T)}{S_{-1}(m,T)} \to 0. \tag{D45}$$

As a result dividing both numerator and denominator by $S_{-1}(m,T)$ in g,

$$\lim_{\beta m\to\infty} g = \lim_{\beta m\to\infty} \frac{\frac{A(m,T)}{S_{-1}(m,T)}\ln\mu + \frac{B(m,T)}{S_{-1}(m,T)}}{\frac{C(m,T)}{S_{-1}(m,T)}\ln\mu + \frac{D(m,T)}{S_{-1}(m,T)}} \approx -\left(\frac{\gamma_{m1}}{\gamma_{m2}}\right), \tag{D46}$$

where

$$\lim_{\beta m\to\infty} \frac{A(m,T)}{S_{-1}(m,T)} \approx -\gamma_{m1} \times -\frac{m^4}{2(4\pi)^4}\left[\psi(2) + \ln\left(\frac{4\pi}{m^2}\right)\right], \tag{D47}$$

$$\lim_{\beta m\to\infty} \frac{B(m,T)}{S_{-1}(m,T)} \approx -\gamma_{m1} \times -\frac{m^4}{(4\pi)^4}, \tag{D48}$$

$$\lim_{\beta m\to\infty} \frac{C(m,T)}{S_{-1}(m,T)} \approx \gamma_{m2} \times -\frac{m^4}{2(4\pi)^4}\left[\psi(2) + \ln\left(\frac{4\pi}{m^2}\right)\right], \tag{D49}$$

$$\lim_{\beta m\to\infty} \frac{D(m,T)}{S_{-1}(m,T)} \approx \gamma_{m2} \times -\frac{m^4}{(4\pi)^4}. \tag{D50}$$

Now we have other equations relating μ and g as

$$\ln\left(\frac{\mu}{\mu_0}\right) = \frac{-1}{\beta_2 g} + \frac{\beta_3}{\beta_2^2}\ln\left(\beta_3 + \frac{\beta_2}{g}\right). \tag{D51}$$

When we apply the result Eq. (D46) on the above equations, we get

$$\lim_{\beta m\to\infty} \ln\left(\frac{\mu}{\mu_0}\right) = \frac{\gamma_{m2}}{\beta_2\gamma_{m1}} + \frac{\beta_3}{\beta_2^2}\ln\left(\beta_3 - \frac{\gamma_{m2}\beta_2}{\gamma_{m1}}\right). \tag{D52}$$

At this approximation, at zero momentum limit, the right-hand side of Eq. (D52) goes to a complex number. If we choose μ_0 in the left-hand side accordingly (i.e., to a complex number/complex function approximation at $T \approx 0$), one can still make $\mu(T \approx 0)$ a real number.

The relation between the running mass and the coupling relation at $T \to 0$ approximated is

$$\lim_{\beta m\to\infty} \ln\left(\frac{m}{m_0}\right) = \chi_2 + \frac{\gamma_{m1}}{\beta_2}\ln\left(\frac{-\gamma_{m1}}{\gamma_{m2}}\right) + \left(\frac{\gamma_{m2}}{\beta_3} - \frac{\gamma_{m1}}{\beta_2}\right)\ln\left(\beta_2 - \frac{\gamma_{m1}\beta_3}{\gamma_{m2}}\right). \tag{D53}$$

At this approximation one can choose running mass $m(T \approx 0)$ as real or complex by intentionally choosing χ_2 and $\ln\mu_0$ accordingly.

2. Pressure P limit case $T \to 0$

In Fig. 3, we have chosen different values as T_0, P_0, χ_2, $\ln\mu$. All those results show a similar course, i.e., $T \to \infty$, $P \to P_{\text{ideal}}$, irrespective of the initial value.

The quasiparticle model derives energy density from standard statistical mechanics at relativistic Bose-Einstein distribution, i.e.,

$$\langle\varepsilon\rangle = \int \frac{\sqrt{p^2+m^2}}{\exp(\beta\sqrt{p^2+m^2})-1}\frac{d^3p}{(2\pi)^3}, \tag{D54}$$

$$\langle\varepsilon\rangle = \frac{1}{2\pi^2}\int_0^\infty \frac{p^2\sqrt{p^2+m^2}}{\exp(\beta\sqrt{p^2+m^2})-1}dp. \tag{D55}$$

$$\text{Put} p = m\sinh x \tag{D56}$$

$$= \frac{m^4}{16\pi^2}\int_0^\infty \frac{\cosh(4x)-1}{\exp(\beta m\cosh(x))-1}dx. \tag{D57}$$

At $T \to 0$, i.e., $\beta m \to \infty$, we have

$$\lim_{\beta m\to\infty}\langle\varepsilon\rangle = \frac{m^4}{16\pi^2}\int_0^\infty (\cosh(4x)-1)\exp(-\beta m\cosh(x)) \tag{D58}$$

$$= \frac{m^4}{16\pi^2}(K_4(\beta m)-K_0(\beta m)). \tag{D59}$$

We have

$$\lim_{x\to\infty} K(N,x) \to 0, \qquad \therefore \lim_{\beta m\to\infty}\langle\varepsilon\rangle = 0. \tag{D60}$$

The equation relating pressure with energy is

$$P(T) = \frac{T}{T_0}P_0 + T\int_{T_0}^{T}\frac{\varepsilon(T)}{T^2}dT. \tag{D61}$$

In Eq. (D61) as $T \to T_0$, the integral becomes zero. (The ntegral becomes a zero width integral.) So at $T \to T_0$, $P \to P_0$. One can choose P_0 as negative or positive or zero. We have shown in the figure that irrespective of that the value pressure goes to the ideal limit. In the case of the integrand $\frac{\varepsilon(T)}{T^2}$ at the zero temperature limit, we assume $m \neq 0$, and $T \to 0 \Rightarrow \beta m \to \infty$, according to Eq. (D59),

$$\lim_{\beta m\to\infty}(\beta m)^2 K_N(\beta m) \to 0. \tag{D62}$$

Since energy density at zero temperature limits reaches zero value, there is no point in choosing anything other than zero for P_0 at $T \to 0$. The value of pressure can be made negative at some points if one chooses P_0 as negative at the appropriate T_0. In our case, we found that it reaches the ideal value at a high-temperature limit, whatever may be the initial value.

APPENDIX E: MATSUBARA SUMMATION RESULTS

Here we introduce specific Matsubara summation results involved in calculations we have described earlier, and the symbols have the usual meanings. Here ω_n denotes the $2\pi nT$ where n is the Matsubara frequency and T is the temperature. β indicates the inverse temperature in natural units, i.e., $1/T$:

$$T\sum_{n=-\infty}^{\infty}\frac{1}{\omega_n^2+\varepsilon_p^2} = \frac{1}{2\varepsilon_p}+\frac{n_B(\beta\varepsilon_p)}{\varepsilon_p}, \tag{E1}$$

$$T\sum_{n_p=-\infty}^{\infty}\frac{1}{\omega_{n_p}^2+\varepsilon_p^2}\frac{1}{\omega_{n_p-n_q}^2+\varepsilon_q^2} = [t_1(p,q,n_q)+t_2(p,q,n_q)+t_2(q,p,n_q)], \tag{E2}$$

$$T^2\sum_{n_p=-\infty}^{\infty}\sum_{n_q=-\infty}^{\infty}\frac{1}{\omega_{n_p}^2+\varepsilon_p^2}\frac{1}{\omega_{n_q}^2+\varepsilon_q^2}\frac{1}{\omega_{n_p+n_q+n_r}^2+\varepsilon_r^2} = S_1+S_2+S_3, \tag{E3}$$

$$T^2\sum_{n=-\infty}^{\infty}\sum_{\theta=-\infty}^{\infty}\frac{1}{\omega_n^2+\varepsilon_p^2}\frac{1}{\omega_\theta^2+\varepsilon_q^2}\frac{1}{\omega_{n-\alpha}^2+\varepsilon_r^2}\frac{1}{\omega_{n-\theta+\eta}^2+\varepsilon_s^2} = T^2\sum_{n=-\infty}^{\infty}\sum_{\theta=-\infty}^{\infty}\frac{1}{\omega_n^2+\varepsilon_p^2}\frac{1}{\omega_\theta^2+\varepsilon_s^2}\frac{1}{\omega_{n-\alpha}^2+\varepsilon_r^2}\frac{1}{\omega_{n-\theta+\eta}^2+\varepsilon_q^2} \tag{E4}$$

$$= \frac{T_{s2}^1+T_{s2}^2+T_{s2}^3}{16\varepsilon_p\varepsilon_r\varepsilon_q\varepsilon_s} \tag{E5}$$

with

$$t_1(p,q,n_r) = \sum_{\sigma=\pm1} \frac{1}{4\varepsilon_p\varepsilon_q}\left(\frac{1}{\varepsilon_p+\varepsilon_q+i\sigma\omega_{n_r}}\right), \tag{E6}$$

$$t_2(p,q,n_r) = \sum_{\sigma,\sigma_1=\pm1} \frac{1}{4\varepsilon_p\varepsilon_q}\frac{1}{\sigma_1\varepsilon_p+\varepsilon_q+i\sigma\omega_{n_r}} n_B(\beta\varepsilon_p), \tag{E7}$$

(E8)

$$S_1 = \frac{1}{8\varepsilon_p\varepsilon_q\varepsilon_r}\left(\sum_{\sigma=\pm1}\frac{1}{\varepsilon_p+\varepsilon_q+\varepsilon_r+i\sigma\omega_{n_r}}\right), \tag{E9}$$

$$S_2 = \frac{1}{8\epsilon_p\epsilon_q\epsilon_r}\sum_{\sigma,\sigma_1=\pm1}\left(\frac{n_B(\beta\varepsilon_p)}{\sigma_1\varepsilon_p+\varepsilon_q+\varepsilon_r+i\sigma\omega_{n_r}}+\frac{n_B(\beta\varepsilon_q)}{\varepsilon_p+\sigma_1\varepsilon_q+\varepsilon_r+i\sigma\omega_{n_r}}+\frac{n_B(\beta\varepsilon_r)}{\varepsilon_p+\varepsilon_q+\sigma_1\varepsilon_r+i\sigma\omega_{n_r}}\right), \tag{E10}$$

$$S_3 = \frac{1}{8\varepsilon_p\varepsilon_q\varepsilon_r}\sum_{\sigma,\sigma_1,\sigma_2=\pm1}\left(\frac{n_B(\beta\varepsilon_q)n_B(\beta\varepsilon_r)}{\varepsilon_p+\sigma_1\varepsilon_q+\sigma_2\varepsilon_r+i\sigma\omega_{n_r}}+\frac{n_B(\beta\varepsilon_p)n_B(\beta\varepsilon_q)}{\sigma_1\varepsilon_p+\sigma_2\varepsilon_q+\varepsilon_r+i\sigma\omega_{n_r}}+\frac{n_B(\beta\varepsilon_p)n_B(\beta\varepsilon_r)}{\sigma_1\varepsilon_p+\varepsilon_q+\sigma_2\varepsilon_r+i\sigma\omega_{n_r}}\right), \tag{E11}$$

$$\begin{aligned} T^1_{s2} = &\sum_{\sigma=\pm1}\frac{1}{\varepsilon_r+\varepsilon_p-i\sigma\omega_\alpha}\frac{1}{\varepsilon_p+\varepsilon_q+\varepsilon_s+i\sigma\omega_\eta}+\sum_{\sigma=\pm1}\frac{1}{\varepsilon_r+\varepsilon_p+i\sigma\omega_\alpha}\frac{1}{\varepsilon_r+\varepsilon_q+\varepsilon_s+i\sigma\omega_{\eta+\alpha}} \\ &+\sum_{\sigma=\pm1}\frac{1}{\varepsilon_r+\varepsilon_q+\varepsilon_s+i\sigma\omega_{\alpha+\eta}}\frac{1}{\varepsilon_p+\varepsilon_q+\varepsilon_s+i\sigma\omega_\eta}, \end{aligned} \tag{E12}$$

$$T^2_{s2} = t_{21}+t_{22}+t_{23}+t_{24}+t_{25}+t_{26}+t_{27}+t_{28}, \tag{E13}$$

$$T^3_{s2} = t_{31}+t_{32}+t_{33}+t_{34}+t_{35}, \tag{E14}$$

$$t_{21} = \sum_{\sigma,\sigma_1,\sigma_2=\pm1}\frac{1}{\varepsilon_r+\sigma_1(\varepsilon_p-i\sigma\omega_\alpha)}\frac{1}{\varepsilon_q+\varepsilon_s+\sigma_2(\varepsilon_p+i\sigma\omega_\eta)}n_B(\beta\varepsilon_p), \tag{E15}$$

$$t_{22} = \sum_{\sigma,\sigma_1,\sigma_2=\pm1}\frac{1}{\varepsilon_p+\sigma_1(\varepsilon_r+i\sigma\omega_\alpha)}\frac{1}{\varepsilon_q+\varepsilon_s+\sigma_2(\varepsilon_r+i\sigma\omega_{\eta+\alpha})}n_B(\beta\varepsilon_r), \tag{E16}$$

$$t_{23} = \sum_{\sigma,\sigma_2=\pm1}\frac{1}{\varepsilon_s+\varepsilon_r+\sigma_2\varepsilon_q+i\sigma(\omega_{\eta+\alpha})}\frac{1}{\varepsilon_p+\varepsilon_s+\sigma_2\varepsilon_q+i\sigma\omega_\eta}n_B(\beta\varepsilon_q), \tag{E17}$$

$$t_{24} = \sum_{\sigma,\sigma_2=\pm1}\frac{1}{\varepsilon_r+\varepsilon_p+i\sigma\omega_\alpha}\frac{1}{\varepsilon_p+\varepsilon_s+\sigma_2\varepsilon_q-i\sigma\omega_\eta}n_B(\beta\varepsilon_q), \tag{E18}$$

$$t_{25} = \sum_{\sigma,\sigma_2=\pm1}\frac{1}{\varepsilon_r+\varepsilon_p+i\sigma\omega_\alpha}\frac{1}{\varepsilon_r+\varepsilon_s+\sigma_2\varepsilon_q+i\sigma\omega_{\eta+\alpha}}n_B(\beta\varepsilon_q), \tag{E19}$$

$$t_{26} = \sum_{\sigma,\sigma_2=\pm1}\frac{1}{\varepsilon_q+\varepsilon_r+\sigma_2\varepsilon_s+i\sigma\omega_{\eta+\alpha}}\frac{1}{\varepsilon_p+\varepsilon_q+\sigma_2\varepsilon_s+i\sigma\omega_\eta}n_B(\beta\varepsilon_s), \tag{E20}$$

$$t_{27} = \sum_{\sigma,\sigma_2=\pm1}\frac{1}{\varepsilon_r+\varepsilon_p+i\sigma\omega_\alpha}\frac{1}{\varepsilon_p+\varepsilon_q+\sigma_2\varepsilon_s-i\sigma\omega_\eta}n_B(\beta\varepsilon_s), \tag{E21}$$

$$t_{28} = \sum_{\sigma,\sigma_2=\pm1}\frac{1}{\varepsilon_r+\varepsilon_p+i\sigma\omega_\alpha}\frac{1}{\varepsilon_r+\varepsilon_q+\sigma_2\varepsilon_s+i\sigma\omega_{\eta+\alpha}}n_B(\beta\varepsilon_s), \tag{E22}$$

$$t_{31} = \sum_{\sigma,\sigma_1,\sigma_2,\sigma_3=\pm1} \frac{1}{\varepsilon_r + \sigma_1(\varepsilon_p - i\sigma\omega_\alpha)} \frac{1}{\varepsilon_s + \sigma_2\varepsilon_q + \sigma_3(\varepsilon_p + i\sigma\omega_\eta)} n_B(\beta\varepsilon_p) n_B(\beta\varepsilon_q), \tag{E23}$$

$$t_{32} = \sum_{\sigma,\sigma_1,\sigma_2,\sigma_3=\pm1} \frac{1}{\varepsilon_r + \sigma_1(\varepsilon_p - i\sigma\omega_\alpha)} \frac{1}{\varepsilon_q + \sigma_2\varepsilon_s + \sigma_3(\varepsilon_p + i\sigma\omega_\eta)} n_B(\beta\varepsilon_p) n_B(\beta\varepsilon_s), \tag{E24}$$

$$t_{33} = \sum_{\sigma,\sigma_1,\sigma_2,\sigma_3=\pm1} \frac{1}{\varepsilon_p + \sigma_1(\varepsilon_r + i\sigma\omega_\alpha)} \frac{1}{\varepsilon_q + \sigma_2\varepsilon_s + \sigma_3(\varepsilon_r + i\sigma\omega_{\eta+\alpha})} n_B(\beta\varepsilon_r) n_B(\beta\varepsilon_s), \tag{E25}$$

$$t_{34} = \sum_{\sigma,\sigma_1,\sigma_2,\sigma_3=\pm1} \frac{1}{\varepsilon_p + \sigma_1(\varepsilon_r - i\sigma\omega_\alpha)} \frac{1}{\varepsilon_s + \sigma_2\varepsilon_q + \sigma_3(\varepsilon_r - i\sigma\omega_{\eta+\alpha})} n_B(\beta\varepsilon_r) n_B(\beta\varepsilon_q), \tag{E26}$$

$$t_{35} = \sum_{\sigma,\sigma_1,\sigma_2,\sigma_3=\pm1} \frac{1}{\varepsilon_p + \sigma_2\varepsilon_s + \sigma_1\varepsilon_q + i\sigma\omega_\eta} \frac{1}{\varepsilon_r + \sigma_3(\sigma_2\varepsilon_s + \sigma_1\varepsilon_q + i\sigma\omega_{\eta+\alpha})} n_B(\beta\varepsilon_s) n_B(\beta\varepsilon_q), \tag{E27}$$

$$n_B(x) = (e^x - 1)^{-1}, \tag{E28}$$

$$\beta = 1/T. \tag{E29}$$

[1] V. Goloviznin and H. Satz, Zeit. fr Phys. C **57**, 671 (1993).
[2] A. Peshier, B. Kmpfer, O. Pavlenko, and G. Soff, Phys. Lett. B **337**, 235 (1994).
[3] R. A. Schneider and W. Weise, Phys. Rev. C **64**, 055201 (2001).
[4] P. N. Meisinger, M. C. Ogilvie, and T. R. Miller, Phys. Lett. B **585**, 149 (2004).
[5] V. M. Bannur, Phys. Rev. C **75**, 044905 (2007).
[6] V. M. Bannur, Eur. Phys. J C **50**, 629 (2007).
[7] V. M. Bannur, Phys. Lett. B **647**, 271 (2007).
[8] S. Koothottil and V. M. Bannur, Phys. Rev. C **99**, 035210 (2019).
[9] S. Koothottil and V. M. Bannur, Phys. Rev. C **102**, 015206 (2020).
[10] J. C. Collins and M. J. Perry, Phys. Rev. Lett. **34**, 1353 (1975).
[11] J. I. Kapusta, Phys. Rev. D **20**, 989 (1979).
[12] H. Matsumoto, Y. Nakano, and H. Umezawa, Phys. Rev. D **29**, 1116 (1984).
[13] Y. Fujimoto and H. Yamada, Phys. Lett. B **200**, 167 (1988).
[14] R. Baier, B. Pire, and D. Schiff, Phys. Lett. B **238**, 367 (1990).
[15] H. Nakkagawa and A. Niégawa, Phys. Lett. B **193**, 263 (1987).
[16] H. Nakkagawa, A. Niégawa, and H. Yokota, Phys. Rev. D **38**, 2566 (1988).
[17] M. Chaichian and M. Hayashi, Acta Phys. Pol. B **27**, 1703 (1996).
[18] K. Sasaki, Nucl. Phys. **B490**, 472 (1997).
[19] E. Braaten and R. D. Pisarski, Phys. Rev. Lett. **64**, 1338 (1990).
[20] M. A. van Eijck, C. R. Stephens, and C. G. van Weert, Mod. Phys. Lett. A **09**, 309 (1994).
[21] M. A. van Eijck, D. O'Connor, and C. R. Stephens, in *NATO ASI Series* (Springer, US, 1994), p. 259.
[22] M. A. van Eijck, D. O'Connor, and C. R. Stephens, Int. J. Mod. Phys. A **10**, 3343 (1995).
[23] C. R. Stephens, Int. J. Mod. Phys. B **12**, 1379 (1998).
[24] C. R. Stephens, A. Weber, P. O. Hess, and F. Astorga, Phys. Rev. D **70**, 045024 (2004).
[25] A. Ayala, C. Dominguez, S. Hernandez-Ortiz, L. Hernandez, M. Loewe, D. M. Paret, and R. Zamora, Phys. Rev. D **98**, 031501 (2018).
[26] E. Ferrer, V. de la Incera, and X. Wen, Phys. Rev. D **91**, 054006 (2015).
[27] S. Nadkarni, Phys. Rev. D **27**, 917 (1983).
[28] A. Deur, S. J. Brodsky, and G. F. de Téramond, Prog. Part. Nucl. Phys. **90**, 1 (2016).
[29] R. A. Schneider, Phys. Rev. D **66**, 036003 (2002).
[30] R. A. Schneider, Phys. Rev. D **67**, 057901 (2003).
[31] F. M. Steffens, Braz. J. Phys. **36**, 582 (2006).
[32] M. Kurian and V. Chandra, Phys. Rev. D **96**, 114026 (2017).
[33] M. Kurian, S. K. Das, and V. Chandra, Phys. Rev. D **100**, 074003 (2019).
[34] H. Kleinert and V. Schulte-Frohlinde, *Critical Properties of Phi4-Theories* (World Scientific, Singapore, 2001).
[35] J. I. Kapusta and C. Gale, *Finite-Temperature Field Theory* (Cambridge University Press, Cambridge, England, 2006).
[36] T. Kaneko, Phys. Rev. D **49**, 4209 (1994).

[37] D. O'connor, C. Stephens, and F. Freire, Mod. Phys. Lett. A **08**, 1779 (1993).
[38] R. R. Parwani, Phys. Rev. D **45**, 4695 (1992).
[39] P. Arnold and C. Zhai, Phys. Rev. D **50**, 7603 (1994).
[40] A. Peshier, B. Kmpfer, O. P. Pavlenko, and G. Soff, Phys. Rev. D **54**, 2399 (1996).
[41] A. Peshier, B. Kmpfer, O. P. Pavlenko, and G. Soff, Euro. Phys. Lett. **43**, 381 (1998).
[42] J. Frenkel, A. V. Saa, and J. C. Taylor, Phys. Rev. D **46**, 3670 (1992).
[43] E. Braaten and A. Nieto, Phys. Rev. D **51**, 6990 (1995).
[44] A. I. Bugrij and V. N. Shadura, arXiv:hep-th/9510232v2.
[45] J. O. Andersen, E. Braaten, and M. Strickland, Phys. Rev. D **62**, 045004 (2000).
[46] J. O. Andersen, E. Braaten, and M. Strickland, Phys. Rev. D **63**, 105008 (2001).
[47] C. G. Bollini and J. J. Giambiagi, Il Nuovo Cimento B (1971–1996) **12**, 20 (1972).
[48] G. 't Hooft and M. Veltman, Nucl. Phys. **B44**, 189 (1972).
[49] G. 't Hooft, Nucl. Phys. **B61**, 455 (1973).
[50] N. N. Bogoliubow and O. S. Parasiuk, Acta Math. **97**, 227 (1957).
[51] J. C. Collins, Nucl. Phys. **B80**, 341 (1974).
[52] E. R. Speer, J. Math. Phys. (N.Y.) **15**, 1 (1974).
[53] P. Breitenlohner and D. Maison, Commun. Math. Phys. **52**, 55 (1977).
[54] W. E. Caswell and A. D. Kennedy, Phys. Rev. D **25**, 392 (1982).